Morphological and mechanical properties of human fascia lata and implications for motor performance

人間の大腿部深筋膜の形態的・力学的特性と
身体運動パフォーマンスとの関連性

２０２０年１月

早稲田大学大学院　スポーツ科学研究科

大塚　俊

OTSUKA, Shun

研究指導教員：　川上　泰雄　教授

Table of contents

CHAPTER 5

CHAPTER 1

General Introduction

1.1. Preface

The deep fascia is a fibrous membrane tissue extending from head to toe (Kumka and Bonar, 2012). The deep fascia is connected to underlying muscles through loose connective tissues (e.g. epimysium) and to inter-muscular septa, tendons, and ligaments without any boundary in between (Stecco et al., 2008). Through such connections, the forces produced by the muscle contractions transmit to the deep fascia which is known as the myofascial force transmission (Huijing, 2009; Maas and Sandercock, 2010; Yucesoy, 2010). These myofascial force transmissions could induce differences in the characteristics of the fascial tissues at different regions of the body. Indeed, the thickness and fiber orientations of the deep fascia are different between sites of the body (e.g. pectoral vs. femoral regions) (Stecco et al., 2009a). In addition, Henderson et al. (2015) performed tensile test on the animal deep fascia and revealed that the mechanical properties of the deep fascia show site-specificity. The muscle architecture (e.g. pennation angles, fascicle length, and volumes) is different according to the sites (Ema et al., 2016; Cutts and Seedhom, 1993). It is therefore presumed that the morphological and mechanical properties of the deep fascia vary depending on the site by the diverse characteristics of the underlying muscles. In addition, several recent studies demonstrated that the deep fascia shows anisotropic mechanical properties (stiffer in the longitudinal than transverse direction) (Stecco et al., 2014; Henderson et al., 2015). It is supposed that these site-specific and anisotropic characteristics of the deep fascia play an important role in human motor performance. However, there have been very few researches which investigated the morphological and mechanical properties of the human deep fascia in detail. Additionally, most of the studies of deep fascia used postmortem human and animal cadavers thereby, interactions between muscles and deep fascia in voluntary motor performance have not been observed.

Direct observation on human cadavers showed that the deep fascia at the thigh region (fascia lata) was thicker compared with other sites (Stecco et al., 2008). The lateral site of the fascia lata is called iliotibial band (ITB) which is mainly composed of the longitudinally directed

collagen fibers. Human ITB is developed compared with other anthropoids (e.g. chimpanzee), suggesting adaptation of ITB to bipedal locomotion (Eng et al., 2015a; Pontzer, 2007). Several studies reported the unique functions of ITB for example, elastic energy storage (Eng et al., 2015b), dynamic joint stability (Schipplein and Andriacchi, 1991), and postural stability (Evans, 1979). ITB originates from the tensor fascia lata and gluteal maximus muscles, and inserts into the Gardy's tubercle of the tibia (Evans, 1979; Vieira et al., 2007), implying ITB length is a function of both hip and knee joint angles. To date, the morphological and mechanical properties of ITB have been examined using human cadavers (Birnbaum et al., 2004; Wilhelm et al., 2017), and only a few studies attempted to measure its characteristics (e.g. thickness) *in vivo* by the magnetic resonance imaging (MRI) and ultrasonography (Gyaran et al., 2011; Gaudreault et al., 2018). Although Tateuchi et al. (2016) reported that the alteration of the ITB stiffness according to postural changes, it is still unclear whether ITB changes its mechanical property by the configurations of hip and knee joint angles. Further, several studies reported that the ITB related injury (ITB syndrome) is induced especially in the distal site of ITB (Orchard et al., 1996; Noble et al., 1980). The major factor of this injury has been suggested to be repetitive compressive/shear stress on ITB over the lateral femoral epicondyle during knee extension and flexion (Orchard et al., 1996; Noble et al., 1980). A recent study reported that ITB syndrome occurs not only at the distal but also the proximal site of the thigh (Decker and Hunt, 2018), suggesting a mechanism other than the above for the injury, and its site-specificity. However, most previous studies focused only on the distal site (e.g. superior border of the patella (Tateuchi et al., 2015, 2016)) of ITB, and the site-dependence of morphological and mechanical properties of ITB has not been examined.

In this thesis, a cadaveric study was conducted to examine the dependence of the morphological and mechanical properties of human deep fascia on the site of the body and tensile direction. *In vivo* studies were also performed to clarify the mechanical interaction between muscles and deep fascia during joint movements. Furthermore, the effect of site- and joint angle-changes on the morphological and mechanical properties of ITB was measured both in cadaveric and *in vivo* conditions.

1.2. Terminology

Deep fascia

Fascia is the general term of the connective tissues from endomysium to dense connective tissues (e.g. organ capsules, muscular septa, ligaments, retinacula, aponeuroses, tendon, deep fascia, and neuro-fascia). In the present thesis, a fibrous membrane tissue which exists between adipose tissues and muscles is defined as the deep fascia.

Morphological properties

The term "morphology" represents the form and structures of an organism. In this thesis, the thickness and fiber orientations of the tissues are used as the index of the morphological properties.

Mechanical properties

The deep fascia and ITB have the elastic and viscoelastic features. The stiffness, Young's modulus, and hysteresis which calculated from the tensile test and the shear wave velocity (SWV) from *in vivo* experiment are used to explain the mechanical properties of the fascial tissues and muscles.

Site-dependence

In this thesis, the differences between sites (inhomogeneity) of the tissues are expressed as site-dependent differences. For example, the specimens of the deep fascia were dissected from the anterior, lateral, medial, and posterior sites, and the morphological and mechanical characteristics between sites were compared in chapter 2.

Direction-dependence (Anisotropy)

The difference of the mechanical properties depending on the tensile direction is defined as direction-dependent difference or anisotropic feature. In chapter 2, the deep fascia was stretched both in the longitudinal and transverse directions to examine the anisotropic mechanical properties. In this thesis, the longitudinal direction is defined as the direction of muscle

contraction, and the transverse direction as the orthogonal to it.

Ex situ

  The measurement using cadaveric specimens was defined as the *ex situ* study. *Ex situ* study was performed in chapter 2 and chapter 4.

In vivo

  The experiment on the living humans as subjects was defined as the *in vivo* study. In the thesis, *in vivo* studies were conducted which are described in chapter 3 and chapter 4.

1.3. Literature review

In this section, previous researches related to deep fascia and ITB are summarized from the views point of their morphological and mechanical properties, and the relationship between fascial tissues and skeletal muscles.

1.3.1. The deep fascia

Most of the organs (e.g. muscles, nerves, and viscera) are wrapped in and/or connect to the fascial tissues (Benjamin, 2009). Fascia is the general term of the connective tissues from endomysium to dense connective tissues (e.g. organ capsules, muscular septa, ligaments, retinacula, aponeuroses, tendon, deep fascia, and neuro-fascia) (Fig.1-1) (Kumka and Bonar, 2012; Schleip et al., 2012). Above all, the deep fascia is a fibrous membrane tissue which exists between adipose tissues and muscles (Fig.1-2). The deep fascia envelopes all muscles of the body and shows various features according to the regions (Stecco et al., 2011).

1.3.2. Morphological characteristics of the deep fascia

The deep fascia is a dense regular woven connective tissue which is mainly composed of the type I collagen fibers (Kumka and Bonar, 2012). Histological studies demonstrated that the thickness of the deep fascia is different among the regions of the body (Fig.1-3). The deep fascia of limbs (thigh: 0.93 mm, lower leg: 0.92 mm, upper limb: 0.86 mm, forearm: 0.76 mm; Stecco et al., 2008) is thicker than that of pectoral region (0.15 mm; Stecco et al., 2009b). The thickness of the deep fascia is also varied depending on the sites even if it covered the same muscle. For example, the fascia lata (deep fascia at thigh) over the rectus femoris was 0.54 mm at proximal, 0.87mm at medial, and 1.42mm at distal sites, and pectoral fascia over the major pectoral muscle was 0.13mm at subclavear, 0.18 mm at mammary, and 0.58 mm at inferior thorax regions, respectively (Stecco et al., 2009a, b).

Stecco et al. (2008) performed histological test and showed that the deep fascia of the limb is composed of two to three layers (0.23 mm for each layer) of parallel collagen fibers with different orientations (Fig.1-4). The bundles of collagen fibers at each layer are lined in the same direction and the angle of the fibers between adjacent layers is approximately 70-80˚ (Benetazzo

6

et al., 2011). Marshall (2001) noted that the thickness and fibers' orientation of the fascial tissues mirror the forces generated by muscular action. From the anatomical observation, fascial fibers were shown to run along especially in the direction of the underlying muscle's contraction (e.g. quadriceps, biceps femoris, semimembranosus, and two heads of gastrocnemius muscles) (Stecco and Stecco, 2012) (Fig.1-5). Architectures and functions of the muscles are different depending on the regions of the human body, therefore, the morphological properties of the deep fascia may be greatly affected by the characteristics of the underlying muscles. However, there have been few studies which investigated the morphological properties of the human deep fascia in detail. Thereby, it remains unclear whether the thickness and fiber orientation of the deep fascia show site-specificity even if it is in the same segment of the body.

1.3.3. Mechanical properties of the deep fascia

The deep fascia shows unequal behavior when it is loaded in the direction of the muscle contraction or its perpendicular direction (Stecco et al., 2009c; Stecco et al., 2014; Henderson et al., 2015). Stecco et al. (2009b) stained cadaveric deep fascia and found that the layer of deep fascia is partly overlapped to the neighboring layers and partly independent (Fig.1-6). These structures of the fascial layers could generate the heterogeneous mechanical properties of the deep fascia. They also suggested that the differences of the fibers' orientation at each layer might induce the direction-dependent (anisotropic) mechanical properties of the deep fascia. Several studies tested viscoelastic properties of the deep fascia which subjected to human and animal cadavers. For example, Henderson et al. (2015) performed bi-axial tensile tests on the canine fascia lata and thoracolumbar fascia in both longitudinal and transverse directions. The maximum load, energy to break, and elastic modulus of the canine deep fascia was different depending on sites and tensile directions (Fig.1-7). Stecco et al. (2014) performed a pilot test on the human crural fascia (only subjected single cadaver's leg) which showed site- and direction-dependent elastic properties of the crural fascia (Fig.1-8). The fascia lata was approximately two times stiffer than that of the thoracolumbar in canine (Henderson et al., 2015), and the anterior site of the human crural fascia was about 1.5 times stiffer compared with the posterior region (Stecco et al., 2014). Additionally, in both studies, deep fascia was stiffer when it loaded in the longitudinal (canine: 71.0-128.2 N

(Maximum load to break), human: 38.6-51.2 N/mm (stiffness)) than in the transverse direction (canine: 29.4-55.3 N (Maximum load to break), human: 13.4-23.6 N/mm (stiffness)). It is presumable that the mechanical properties of the deep fascia are different among regions due to the architectures and functions of the underlying muscles. Nevertheless, most of the studies targeted on the animal cadavers and only a few studies examined the deep fascia of the human cadaver (Stecco et al., 2014; Birnbaum et al., 2014; Wilhelm et al., 2017). Therefore, it is necessary to clarify the mechanical properties of the human deep fascia and the relationships between fascial characteristics and neighboring muscle's functions (Krause et al., 2016).

1.3.4. *In vivo* experiment

Except for using cadavers, there was no other way to examine the morphological and mechanical characteristics of the human deep fascia, to the last decade. With the development of the technology in the last few years, it has become possible to measure the fascial structures *in vivo* (Fig.1-9). Indeed, there are not a lot of, but several studies attempted to measure the morophological and mechanical properties of the human deep fascia *in vivo*. Wilke et al. (2018) measured the thickness of the deep fascia of young and old healthy females taken from six sites of the body (anterior/posterior sites of lower leg and thigh, lumber, and abdominal wall) using Brightness mode (B-mode) images of a high-resolution ultrasonography. The thickness of the deep fascia was thicker in young adults (0.73-0.95 mm) than elderies (0.62-0.83 mm) at most of the sites (anterior/posterior sites of lower leg, anterior thigh, and abdominal wall). Also, they found that the thickness of the deep fascia at some regions (e.g. posterior thigh, abdominal wall, and lumbar) was correlated with the BMI and flexibility (both positive and negative correlation depending on the sites). Another case study tried to measure the stiffness of the deep fascia at lower leg using ultrasound elastography and demonstrated that the deep fascia became more compliant after manual therapy (Luomala et al., 2014) (Fig.1-10). However, at present, there is a paucity of data on the contraction level-dependence of the elastic properties of the deep fascia and its site-differences *in vivo,* and the mechanical interaction between muscles and deep fascia during body movement still remains to be determined.

1.3.5. Interactions between deep fascia and muscles

Skeletal muscles directly insert on and/or connect with the deep fascia through loose connective tissues (e.g. epimysium) (Stecco et al., 2008). These anatomical connections allow fascial tissues to bear forces produced by muscle contractions in an effect to transmit the forces to the neighboring tissues (Huijing et al., 2007; Marshall, 2001). Huijing et al. (2003) demonstrated that around 70% of muscle tension transmits to the tendons, and 30% of muscle force transmits to the connective tissues covering skeletal muscles. These connections between deep fascia and muscles are known as the myofascial force transmission (Huijing, 2009; Maas and Sandercock, 2010; Yucesoy, 2010). Several researchers found that these force transmissions occur in the human body (e.g. lower limb, thoracolumbar, upper limb, etc.) through various connective tissues including deep fascia (Huijing et al., 2011; Carvalhais et al., 2013; Marinho et al., 2017; Yoshitake et al., 2018). The force transmissions occur not only between synergists but also antagonists (Maas and Sanderock, 2010; Huijing et al., 2007). Findley et al. (2015) simulated that muscle force generated by muscle contraction transmits both longitudinally and radially (Fig1-11). These previous studies pointed out that the deep fascia receives mechanical load which is induced not only by the longitudinal muscle contraction but due to the radial deformation and bulging. It is expected that the fascial structures play a role in transmitting the forces produced by the underlying muscles to their neighboring muscles, but little has been clarified so far.

1.3.6. Fascial related therapies

Due to the connections between fascial tissues and muscles, there is a focal point of the fascia where the force produced by the muscles' contraction concentrates on (Stecco et al., 2013). From the clinical practice, it is known that the location of the concentration of the force correlates with movement dysfunction and distribution of symptoms (Day et al., 2012; Stecco et al., 2013). Therefore, manipulation of these areas could contribute to swift restoration of normal movement (Day et al., 2012). Several treatment methods approaching to the fascial tissue were used in the clinical field (e.g. Fascial tissue therapy, connective tissue manipulation, myofascial release and fascial manipulation) (Lambert et al., 2017). There are several studies which have proven the effects of these methods for the chronic pain and limited joint range of motion (table 1-1). For

example, Ichikawa et al. (2015) showed that the gliding motion of the deep fascia over VL was increased (flexibility was improved) after the myofascial release (Fig.1-12a). Ikeda et al. (2019) performed instrument-assisted soft tissue mobilization on the lower leg and revealed the increasing of ankle range of motion without changing muscle stiffness (Fig.1-12b). These studies imply that such manipulations targeting to the fascial tissue as well as muscles contribute to reduce myofascial pain and improve joint mobility. However, most of these methods are merely based on the clinical experience of the clinicians, and it remains unclear whether these manipulations are applied to the proper site- and direction-dependent characteristics of the fascial tissues. The detailed explication of the structural and functional properties of the deep fascia would contribute to develop the manipulation techniques which are corresponding to the characteristics of the deep fascia at each site and help improving the accuracy and efficacy of these manipulation methods.

1.3.7. Morphological and Mechanical properties of Iliotibial band

Iliotibial band (ITB) is the lateral thick part of the fascia lata, being composed mainly of the longitudinally oriented collagen fibers (Kaplan et al., 1958). ITB originates from the tensor fascia lata (TFL) and gluteal maximus (GM) muscles (Evans, 1979), and inserts into the lateral femoral epicondyle, patella, and Gardy's tubercle of the tibia (Vieira et al., 2007). Human ITB is developed compared with other mammals (e.g. chimpanzee), suggesting adaptation for bipedal locomotion (Eng et al., 2015a; Pontzer, 2007). Several studies reported the unique functions of ITB for example, elastic energy storage (Eng et al., 2015b), dynamic joint stability (Schipplein and Andriacchi, 1991), and postural stability (Evans, 1979). Due to its difficulty of the measurement of ITB *in vivo*, the material and mechanical properties of ITB have commonly examined using human cadavers (Birnbaum et al., 2004; Wilhelm et al., 2017). Wilhelm et al. (2017) performed tensile test on the whole ITB-TFL complex (applied 3.75% elongation from initial length) (Fig.1-13) and found that the strain of the proximal site of ITB (4.5 ± 1.8%) was greater than that of the middle (1.4 ± 1.0%) and distal sites (1.7 ± 1.0%). Few studies attempted to measure the characteristics (e.g. thickness) of ITB *in vivo* by magnetic resonance imaging (MRI) and ultrasonography (Gyaran et al., 2011; Gaudreault et al., 2018). According to the

measurement using ultrasonography, the ITB thickness at the level of the lateral femoral epicondyle was 0.8-1.4 mm (Gyaran et al., 2011) (Fig.1-14). There was no significant correlation between the ITB thickness and age, weight, height, dominant limb, and the volume of exercise habit of the participants (Gyaran et al., 2011). To date, there are limited studies which examined the site-dependent mechanical properties of ITB in detail. In addition, some studies revealed the alteration of the stiffness of ITB at the superior boarder of the patella due to the postural changes (e.g. pelvic or trunk inclination, hip extension or flexion, and hip abduction or adduction) during one leg standing (Tateuchi et al., 2015, 2016). These studies implying that the ITB length is the function of both hip and knee joint angles. However, there are insufficient data on the site-dependence of ITB stiffness and its alteration associated with the knee and hip joint configurations.

1.3.8. ITB related injuries

As mentioned in the previous section, it can be considered that ITB plays an important role during our body movement. On the other hand, greater mechanical stress might be developed to ITB due to the various functions of the attached muscles (e.g. TFL, GM, and VL). Repetitive strain injuries are therefore likely to occur at ITB even in the whole deep fascia structure in the lower leg. ITB syndrome is one of the most common overuse injuries inducing lateral knee pain especially in the long-distance runners and cyclists (Holmes et al., 1993; Merlo and Migliorini, 2016). Some review articles noted that 6-52% of the injuries in the long-distance runner and 24% in the cyclists were related to ITB disability (Noble, 1980; Holmes et al., 1993). The major factor of this injury is suggested to be repetitive compressive stress on ITB over the lateral femoral epicondyle during knee extension and flexion (Orchard et al., 1996; Noble et al., 1980). Fairclough et al. (2006) found that the tension in the ITB shifts anterior to posterior of its fibers and ITB stiffness increases when knee being at 20-30° due to against the lateral epicondyle. A recent study reported that ITB syndrome occurs not only at the distal site but also the proximal site of the thigh (Decker and Hunt, 2018), which indicates that the injury of ITB is induced site-specificity. However, most of the studies only focused on the distal site (e.g. superior border of the patella (Tateuchi et al., 2015, 2016)) of ITB, and the site-dependent material and mechanical properties on ITB has not been examined. Fairclough et al. (2007) also claimed that ITB syndrome

is related to impaired function of the hip muscles. In fact, the ITB length is a function of both hip and knee joint angles, thus the joint angle configurations may affect the mechanical properties of ITB. A previous study showed that the stiffness of ITB is increased by the hip extension so that being associated with ITB syndrome (Tateuchi et al., 2016). However, the effect of the combination of both knee and hip joint angles on ITB mechanical properties still remains unclear.
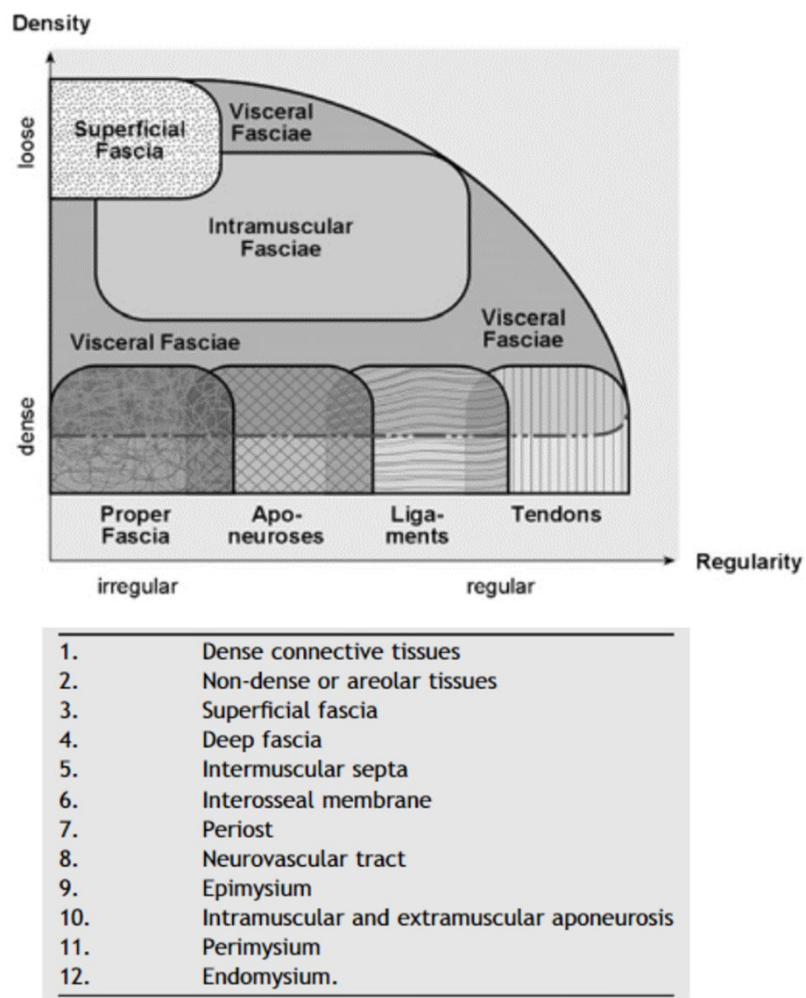
1.3.9. Methods for the measurement of the mechanical properties of soft tissues

To measure the mechanical properties of the soft tissues, several methodologies were performed in the previous studies. The tensile test has been mainly used to measure the mechanical properties of the cadaveric tendons (Bennett et al., 1986; Proske and Morgan, 1987; Maganaris and Paul, 2000), ligaments (Woo et al., 1986), and aponeuroses (Azizi and Roberts, 2009; Shan et al., 2019), and deep fascia (Stecco et al., 2014; Henderson et al., 2015) (Fig. 1-12). From the slope of the relationships between tensile length (mm) and load (N) during tensile test, the stiffness (N/mm) can be calculated. The stiffness represents how much is the tissue difficult to deform in the tensile direction. Therefore, higher stiffness means that the tissue is stiffer. The Young's modulus is the index of elasticity of a substance, expressing the slope between strain (%) and stress (N/mm^2) (strain = changes of length (mm) / initial length (mm), stress = load (N) / CSA of the specimen (mm^2)). As the viscoelastic property of the tissue, the mechanical hysteresis (%) can be calculated from the stress-strain relationship of the loading-unloading cycle (Maganaris and Paul, 2000). The energy required to stretch the tissue (WS) and the energy released by the shortening of the tissue (WR) were calculated by integrating numerically the function of displacement upon loading and unloading, respectively. The mechanical hysteresis in the loading-unloading cycle was calculated as 100 (WS - WR) / WS (Maganaris and Paul, 2000).

For the last several decades, the attempts to measure the elastic properties of the soft tissue *in vivo* are developing. The stiffness, Young's modulus, and hysteresis became able to be measured from the length changes of muscle-tendon unit and torque relationships by the B-mode ultrasonography (Fig. 1-15). To date, such mechanical properties of human muscle-tendon complex were measured to the various targets including children (Mogi et al., 2013, 2018), elderlies (Stenroth et al., 2012), and athletes (Kubo et al., 2000). The effects of the training (Kubo
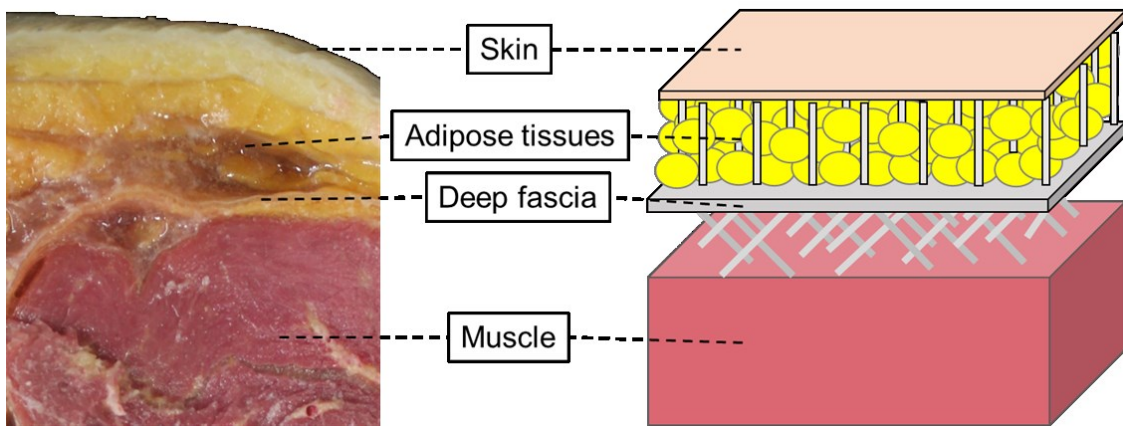
et al.,2001a, 2006), stretching (Kubo et al., 2001b), and exercise (Fukunaga et al., 2002) on tendon viscoelastic properties were also examined using B-mode ultrasonography (Mogi et al., 2018).

Recently, ultrasound shear wave elastography (SWE) which is a new ultrasonography technology has been developed to measure the mechanical properties of the soft tissues *in vivo* non-invasively. By obtaining the propagation speed of shear wave through the tissues, the stiffness of the tissue can be quantified (Arda et al., 2011; Shiina et al., 2015) (Fig. 1-16). The stiffness of the muscles has been examined using SWE in various conditions (e.g. at rest, during and after exercise) (Lacourpaille et al., 2012; Yoshitake et al., 2014, Ateş et al., 2015; Andonian et al., 2016). Collagen-rich tissues for example, tendon, ligament, and plantar fascia have also been examined using SWE (Aubry et al., 2013; Brum et al., 2014; Wu et al., 2012; Wu et al., 2011; Shiotani et al., 2019). However, at present there is paucity of data of the morphological and mechanical properties of the deep fascia and its site-differences *in vivo*. The association between fascial characteristics and human motor performance also remains unclear.

Density

loose

Superficial
Fascia

Visceral
Fasciae

Intramuscular
Fasciae

Visceral Fasciae

Visceral
Fasciae

dense

Proper
Fascia

Apo-
neuroses

Liga-
ments

Tendons

Regularity

irregular

regular

1.	Dense connective tissues
2.	Non-dense or areolar tissues
3.	Superficial fascia
4.	Deep fascia
5.	Intermuscular septa
6.	Interosseal membrane
7.	Periost
8.	Neurovascular tract
9.	Epimysium
10.	Intramuscular and extramuscular aponeurosis
11.	Perimysium
12.	Endomysium.

Fig. 1-1.

Specifying terms for the description of fascial tissues (From Schleip et al., 2012).

Fig. 1-2.

Typical pattern of organization of subcutaneous tissues.
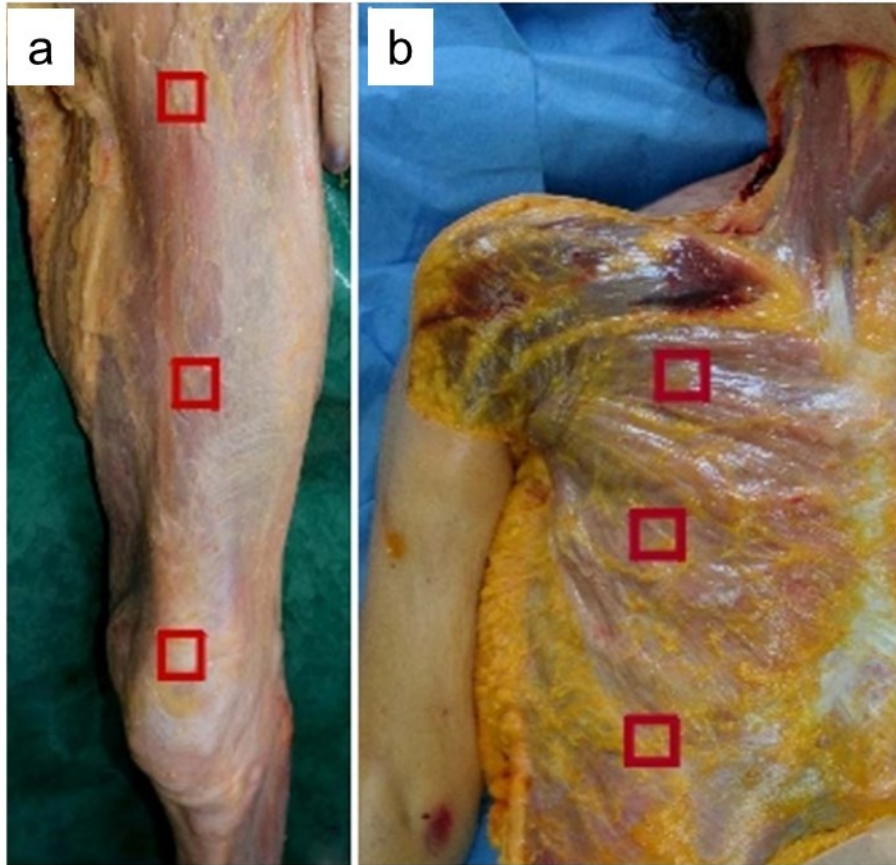
Fig. 1-3.

Deep fascia at the femoral (a) and pectoral (b) region (From Stecco et al., 2009).
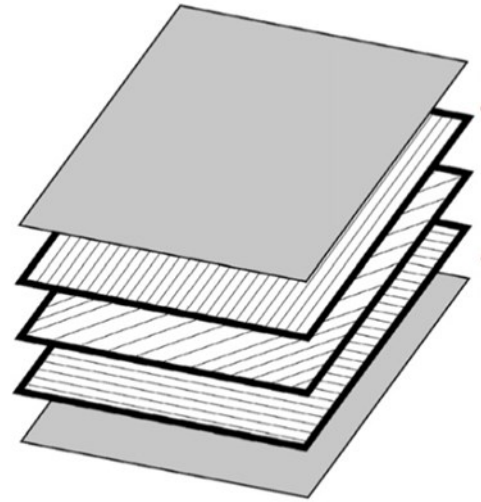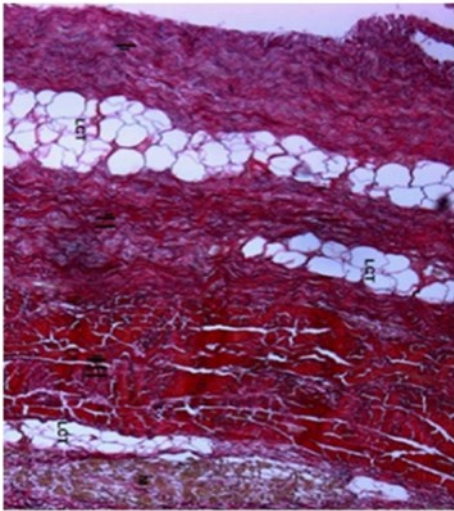
Fig. 1-4.

Histological and schematic images of the deep fascial layers. The deep fascia is composed of two to three layers of parallel collagen fibers (From Stecco et al., 2008)
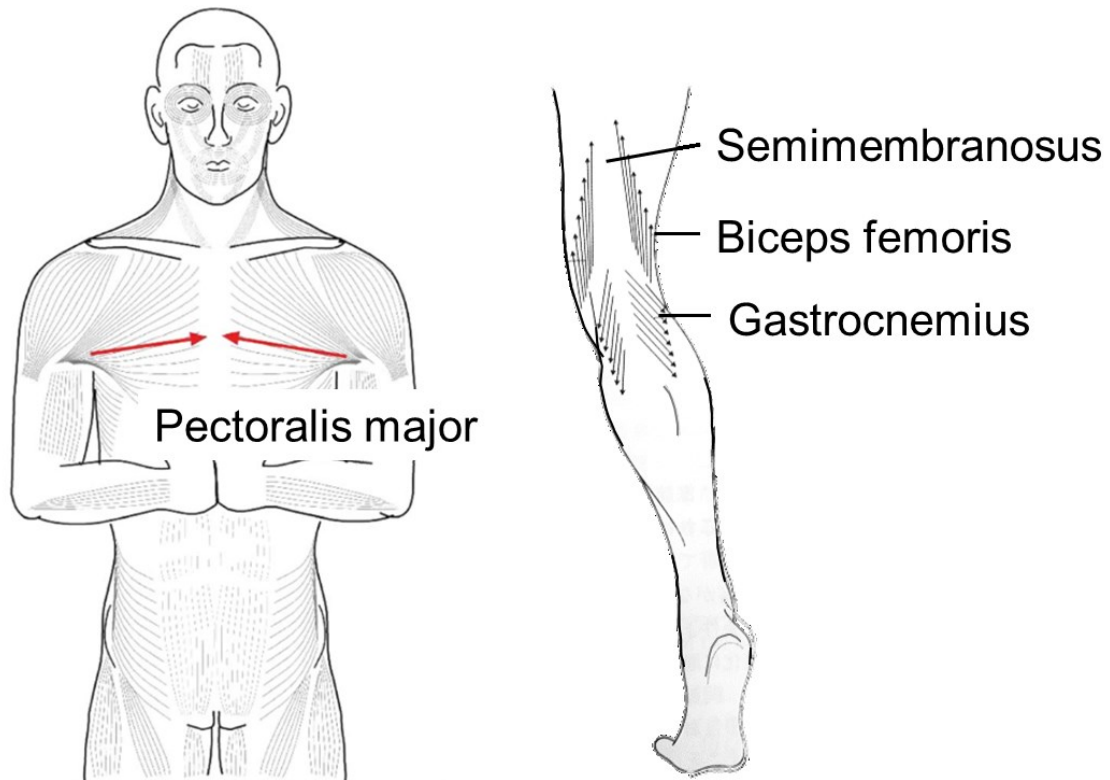
Fig. 1-5.

Fibers' orientations of the fascial tissues mirror the force generated by the action of underlying muscles (From Stecco et al., 2009 and Stecco & Stecco, 2012).
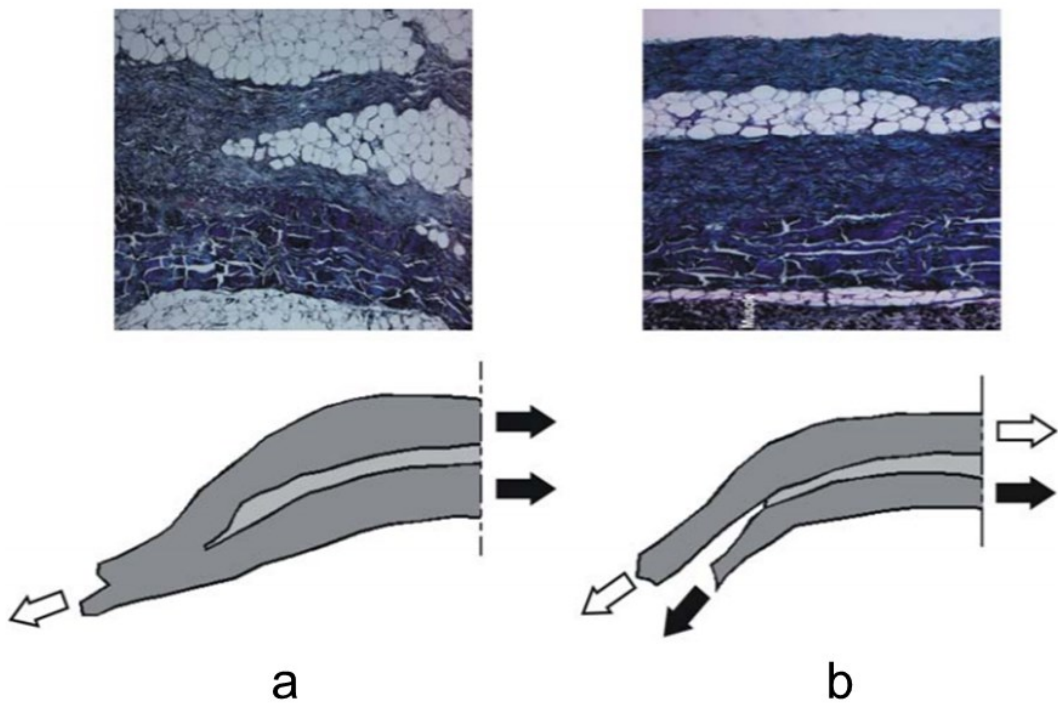
Fig. 1-6.

The laer of deep fascia is partly overlapped to the neighboring layers (a) and partly inependent (b). These characteristics induce heterogeneous mechanical properties of the deep fascia (From Stecco et al., 2009).
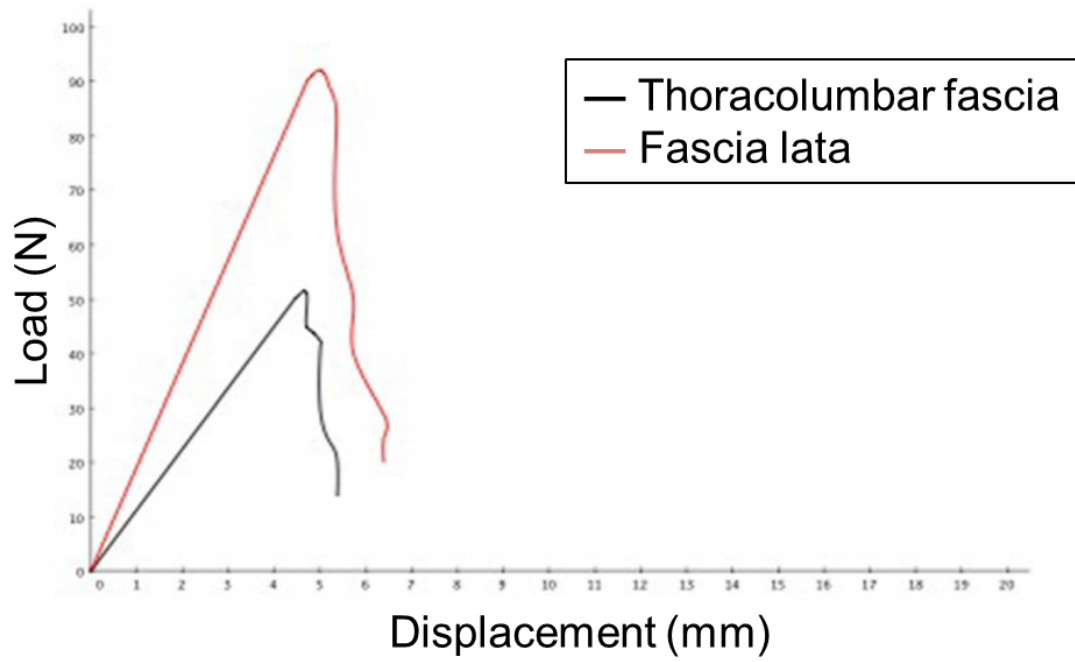
Fig. 1-7.

Mechanical properties of the canine deep fascia. The fascia lata was stiffer than the thoracolumbar fascia (From Stecco et al., 2009, partly modified).
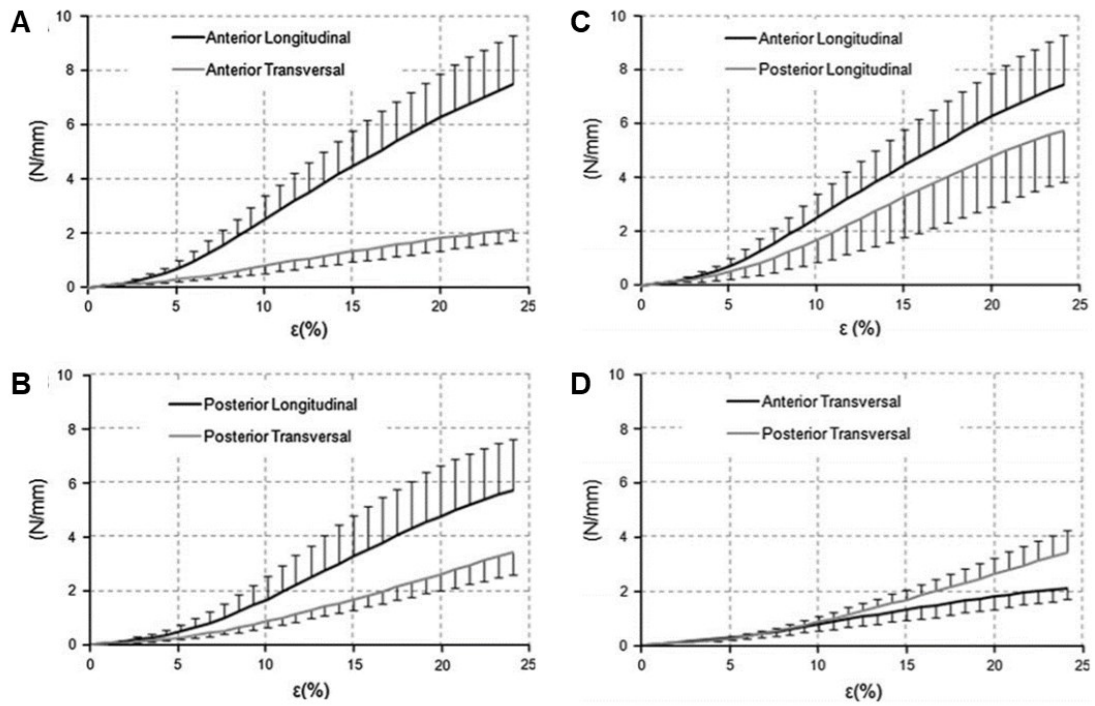
Fig. 1-8.

Mechanical properties of the human crural fascia. The crural fascia was stiffer at the anterior than the posterior site, and stiffer when it stretched in the longitudinal than transverse direction (From Stecco et al., 2009).
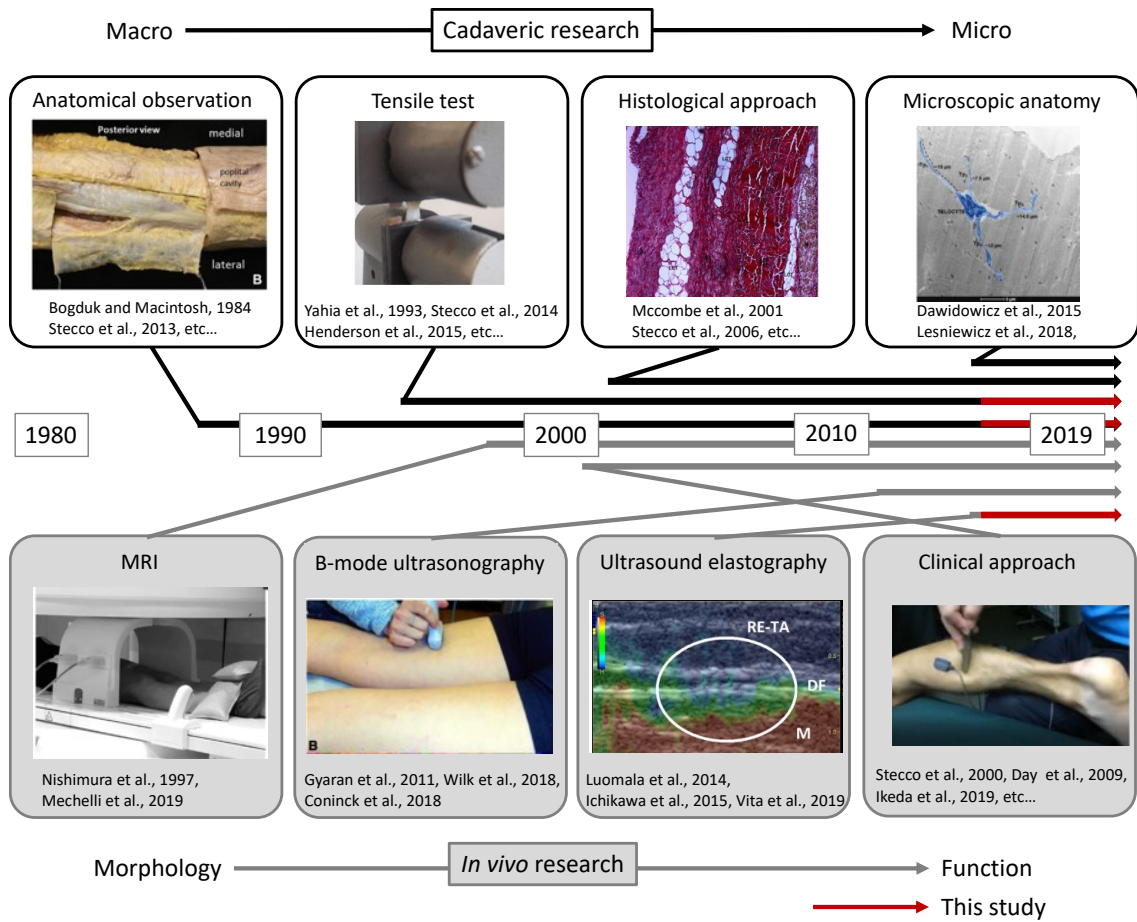
Fig. 1-9.

History of the fascia related research. In recent years, measurements of fascial properties *in vivo* have become possible with the improvement of techniques (From Stecco et al., 2006, 2013, Henderson et al., 2015, Dawidowicz et al., 2015, Mechelli et al., 2019, Wilk et al., 2018, Luomala et al., 2014, and Ikeda et al., 2019).
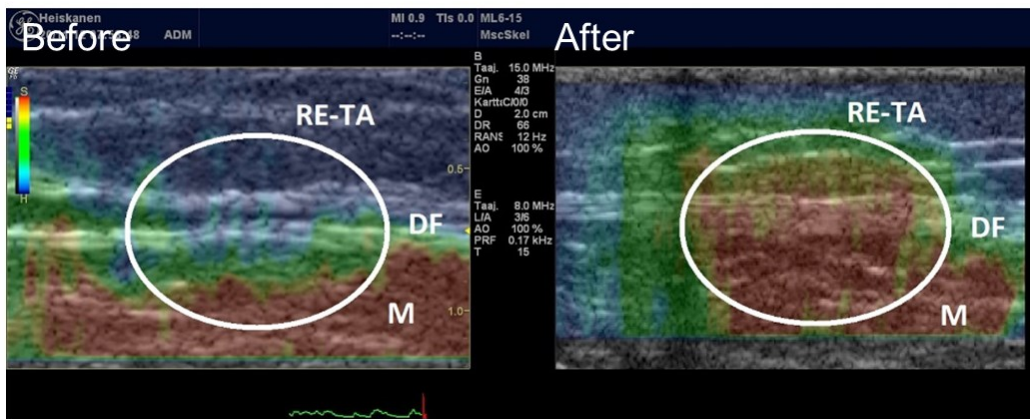
Fig. 1-10.

The image represents the stiffness mapping of the deep fascia. The deep

fascia became more compliant after manual therapy (From Stecco et al.,

2009). DF: deep fascia, M: muscle.

Muscle at Rest

Muscle under contraction

Radial Stress

Force →   ← Force

Radial Stress
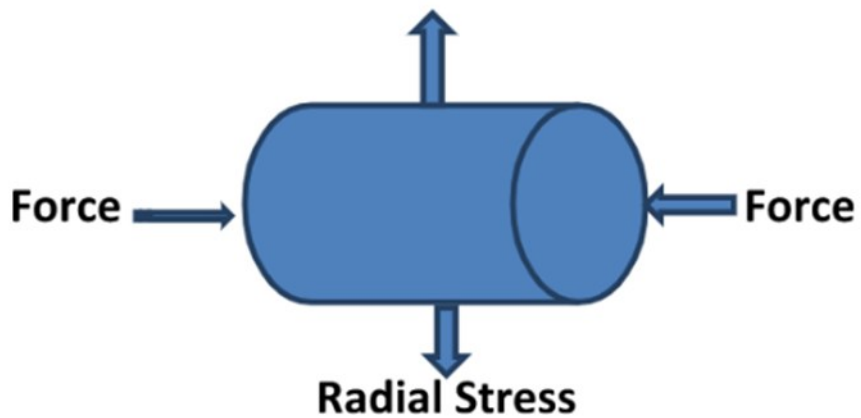
Fig. 1-11.

The force generated by muscle contraction transmits both in the longitudinal and radial directions (From Findley et al., 2015).

Table 1-1. Summary of the effects of the manipulation techniques targeting to fascial tissue

Author	Publish year	Condition	Intervention	Site	Results
Day et al.	2009	28 subjects with chronic posterior brachial pain	Manual therapy (Fascial Manipulation)	scapular region, triceps region, and posterior forearm	VAS for pain -57%
Laudner et al.	2014	17 healthy collegiate baseball players	Instrument-assisted soft tissue mobilization (Graston technique)	posterior shoulder	grenohumeral horizontal adduction ROM +11.1° internal rotation ROM +4.8°
Gulick	2014	49 healthy subjects	Instrument-assisted soft tissue mobilization (Graston technique, pressure dolorimeter)	myofascial trigger points in the upper back	myofascial triggerpoint sensitivity N.S.
Ichikawa et al.	2015	12 healthy males	Manual therapy (Myofascial release)	vastus lateralis	deep fascial motion +40% muscle hardness -30%
Markovic	2015	10 healthy male soccer player	Instrument-assisted soft tissue mobilization (Fascial Abration technique) and Self-myofascial release (Foam rolling)	lower extremity	passive knee flexion ROM +13.1° (FAT), +6.6° (FR) passive hip flexion ROM +15.2° (FAT), +7.0° (FR)
Ikeda et al.	2019	14 healthy young people	Instrument-assisted soft tissue mobilization (Graston technique)	triceps surae muscles and Achilles tendon	dorsiflexion ROM +10.8% joint stiffness -6.2% muscle stiffness N.S.
Harper et al.	2019	56 participants with low back pain	Manual therapy (Fascial Manipulation)	trunk	Oswestry Disability Index -18.4 Numeric Pain Scale -4.3
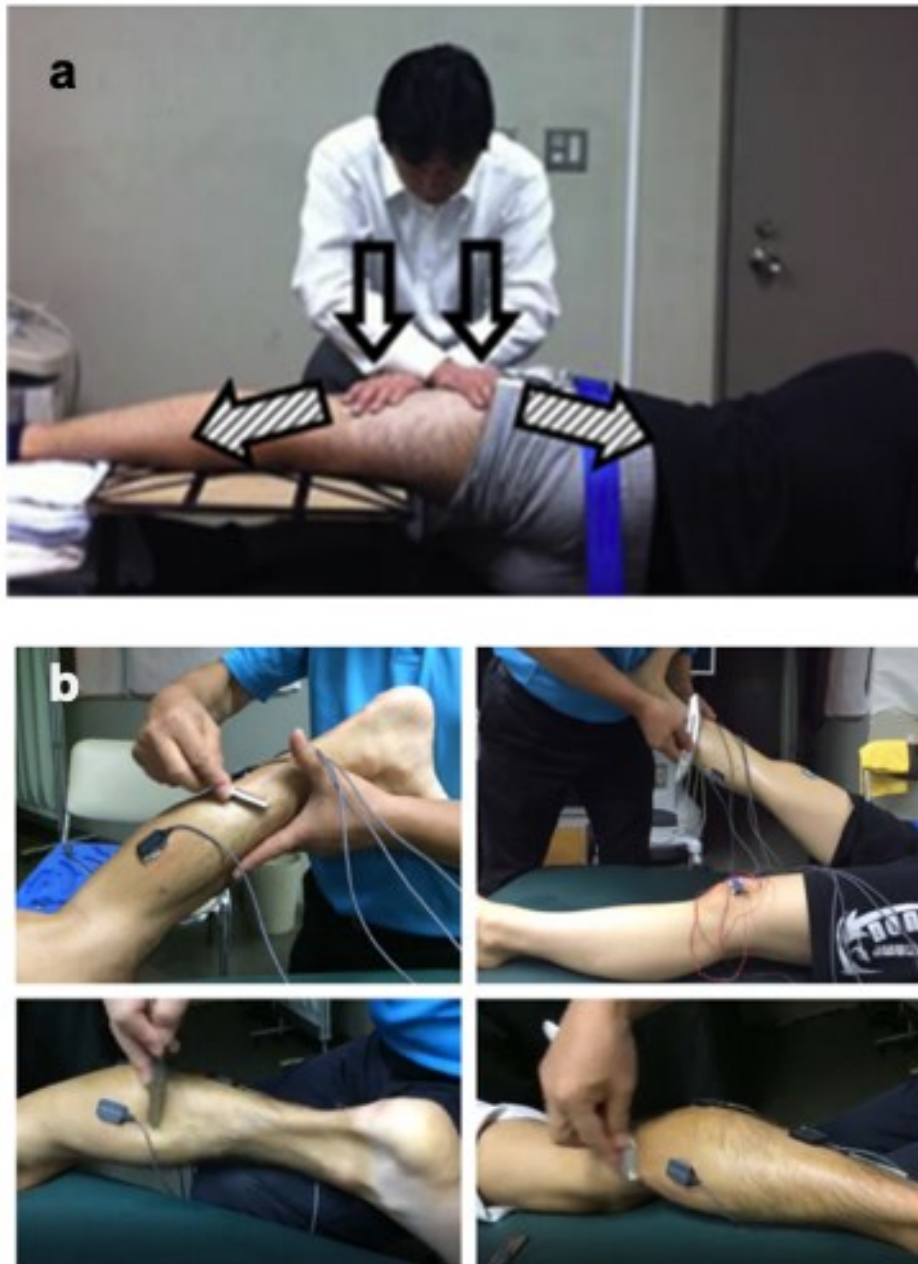
Fig. 1-12.

There are several manipulation methods approaching to the fascial tissues manually (A) and using instruments (B) (From Ichiklawa et al., 2015 and Ikeda et al., 2019).
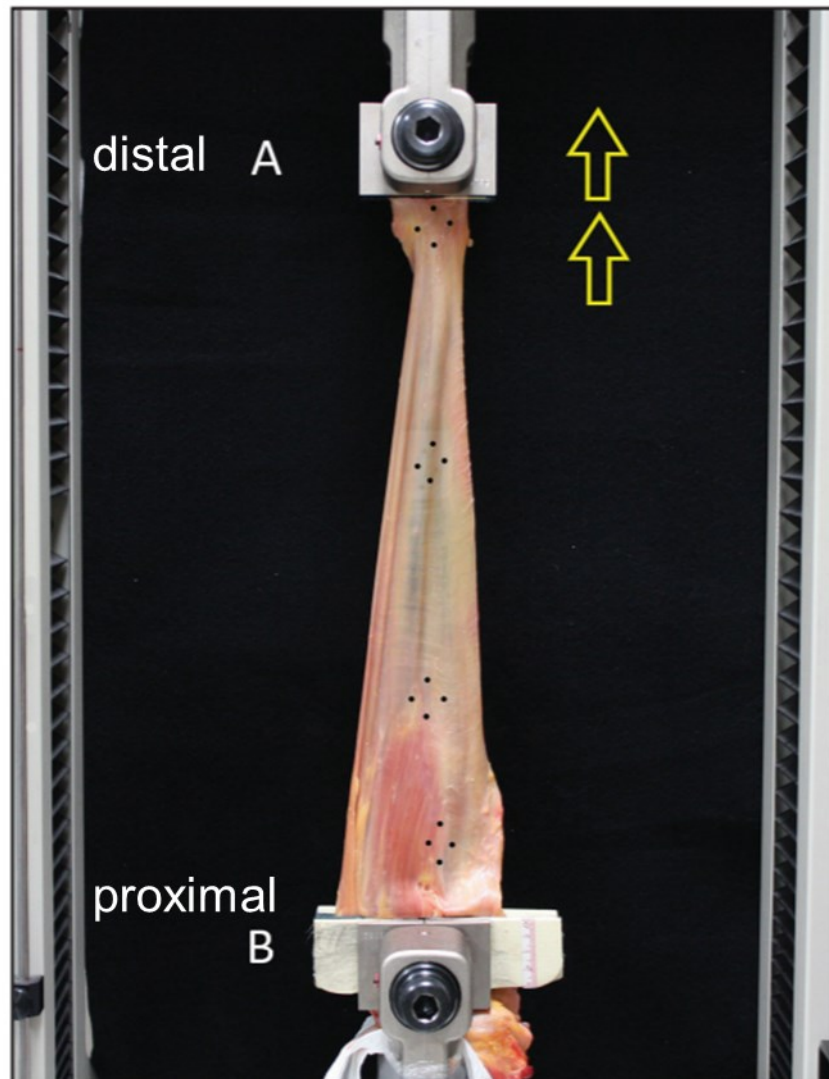
Fig. 1-13.

Findley et al. (2015) performed tensile test on the whole ITB structures
and showed site-specific mechanical properties of ITB (From Findley et
al., 2015).

Fig. 1-14.

Ultrasonographic image of the distal site of ITB. The thickness of ITB was measured from superior boarder of the lateral femoral epicondyle (From Gyaran et al., 2011).
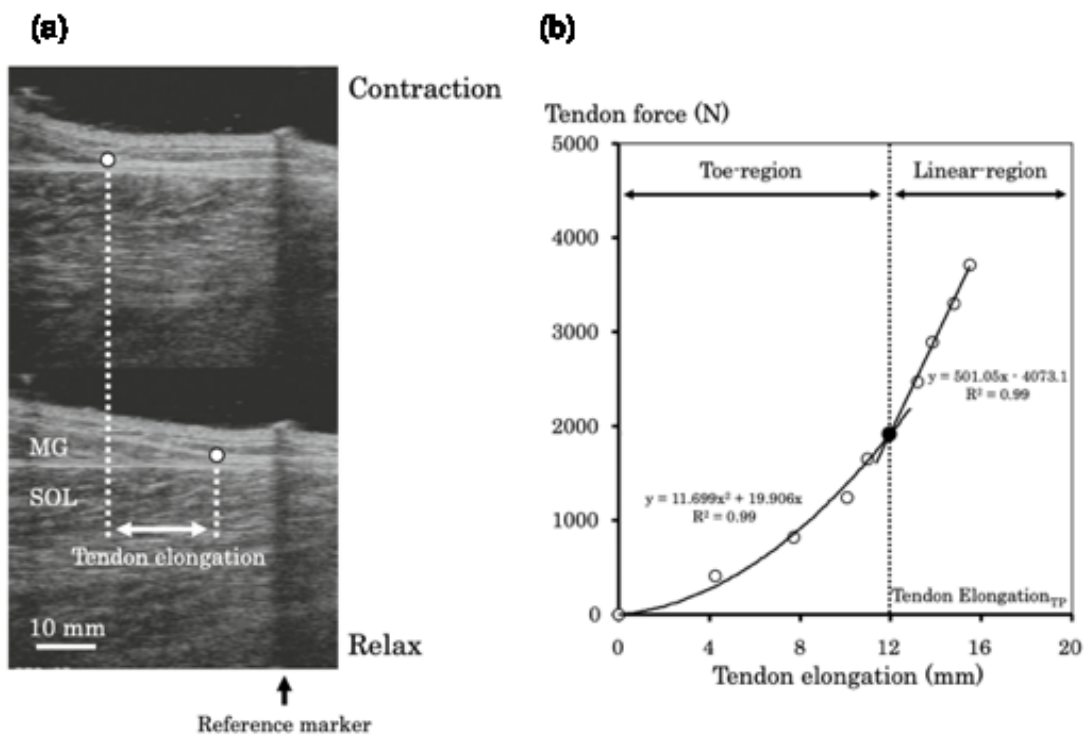
Fig. 1-15.

Ultrasonographic image of muscle-tendon unit (a) and elongation-force relationships of the tendon (b). The mechanical properties were measured from the slope of these relationships (From Mogi et al., 2018).
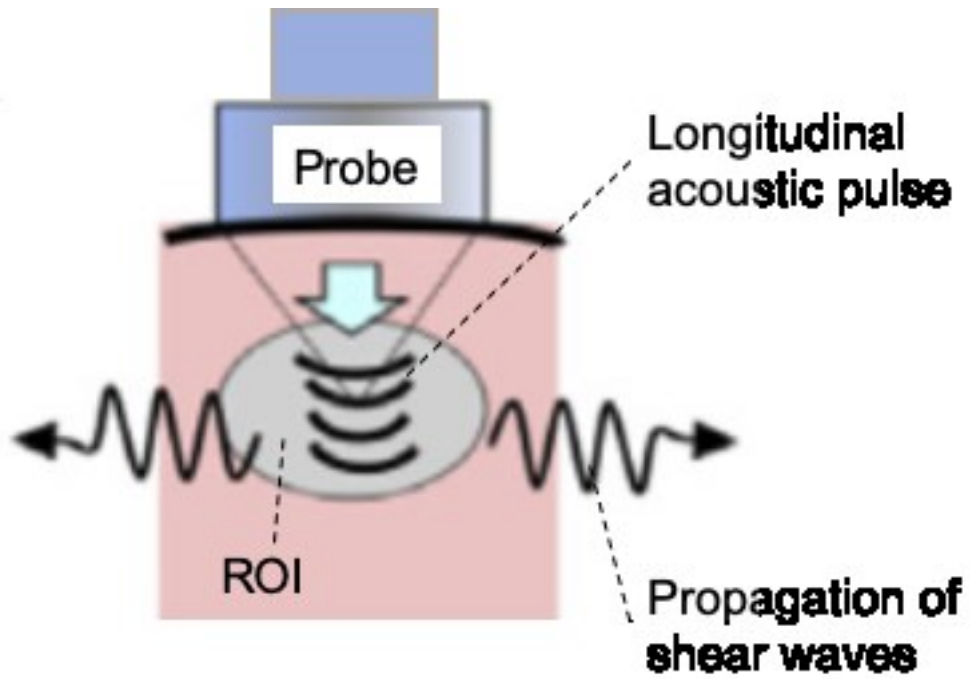
Fig. 1-16.

The general principle of ultrasound shear-wave elastography (From

Shina et al., 2015, partly modified).

1.4. Purpose of the thesis

As mentioned in the literature review, the morphological and mechanical characteristics of the deep fascia and its association with voluntary motor performance remain unclear. It is necessary to combine both cadaveric and i*n vivo* studies for well understanding the characteristics of the fascial structure and its interaction with neighboring muscles. The purposes of the present thesis are to investigate the morphological and mechanical properties of the deep fascia in detail *ex situ* (chapter 2), and the changes of the mechanical properties of the deep fascia during muscle contraction *in vivo* (chapter 3). Additionally, in spite of the outstanding characteristic of ITB among the fascial structures, there are limited numbers of study examined the ITB characteristics in detail. One another purpose of this thesis is to clarify the site- and joint angle-dependence on the mechanical properties of ITB *ex situ* and *in vivo* (chapter 4).

CHAPTER 2

Site-specificity of mechanical and structural properties of human fascia lata and their gender differences: a cadaveric study

2.1. Introduction

As mentioned in the literature review, the deep fascia envelopes skeletal muscles, thereby the characteristics of the underlying muscles may affect the morphological and mechanical properties of the deep fascia. In particular, the thigh is characterized by site- and gender-specific differences of the mass of the skeletal muscles and adipose tissue (Kanehisa et al., 2006; Maruyama et al., 1991). It is therefore presumed that the morphological and mechanical properties of the fascia lata vary depending on the site and gender by such diverse characteristics of underlying muscles. However, there have been few studies on the morphological and mechanical properties of the human fascia lata. The hypothesis was that the morphological properties of the human fascia lata show site- and gender-specificity, which is associated with its mechanical properties.

2.2. Materials and Methods

2.2.1. Specimens preparation

We analyzed the fascia lata at the different sites taken from formalin-fixed human cadavers (17 legs: 9 legs from 6 males and 8 legs from 6 females, 75-92 years). This study's experimental design was approved by the local ethics committee at Aichi Medical University. Specimens of the fascia lata were collected from four sites (anterior, lateral, medial, and posterior) of the 50% of the thigh length (Fig. 2-1). The anterior site was determined so that its mediolateral midpoint corresponded to the center of rectus femoris, and other sites were determined accordingly. The lateral, medial, and posterior sites included portions covering vastus lateralis, gracilis, and semitendinosus respectively. In some samples, the sartorius was partly included in the medial site, so was biceps femoris long head for the posterior site, depending on the muscle sizes of the cadavers. The amount of co-existence of such different muscles was not consistent among samples, but due to the infiltration of adipose tissues between the fascia lata and

underlying muscles, quantification of such variations was not possible in the present study. Each specimen was 40 x 40 mm in the longitudinal (proximal-distal) x transverse (anterior-posterior or lateral-medial) directions. The direction from the greater trochanter to the popliteal fossa was defined as the longitudinal direction and the orthogonal direction to it was defined as the transverse direction. Adipose and connective tissues were manually removed from the specimens using tweezers. After collection, the specimens were stored in a 50 % alcoholic solution at room temperature. The specimens were kept moist throughout the testing (described below) by pipetting them with alcoholic solution. After collection of the specimens, morphological tests were conducted, followed by the mechanical tests.

2.2.2. Morphological tests

Thickness

The thickness of the fascia lata was measured with a digital caliper (LIXIL VIVA, Japan). Briefly, five different points (upper, lower, right, left, and center parts) of the sample were randomly selected at each point, and the average value was calculated as the representative of the thickness of that sample. To avoid the deformation of the tissue due to an applied pressure by the caliper, we used the flat part of the caliper and paid great attention to provide pressure to the sample as small as possible.

Distribution of fiber direction

An image of each specimen's surface was taken by a digital camera (ILEX-QX1, SONY, Japan) adapted to a stereomicroscope (nobita, Micronet, Japan) while radiating light from the back side using a lamp. The image was digitally binarized and the power spectrum was obtained by a fast Fourier transformation (FiberOri8 single03, v.7.10, Japan, Fig. 2-2). The distribution of fiber direction was determined using the same program (Enomae et al., 2005). The fiber direction angle was classified into longitudinal, transverse, and two opposite diagonal directions (Fig. 2-3). Then, the proportion of the fibers in each direction was calculated.

2.2.3. Mechanical tests

Tensile test

To verify the site specificity and anisotropy of the mechanical properties of the fascia lata, a tensile strength test was performed. Specimens of the fascia lata from each region were tested in the longitudinal and transverse directions. Two pieces of sandpapers were adhered to the specimen with tissue glue, which ensured that fascial layers did not slide over each other or out of the clamp when the tissue was loaded (Henderson et al., 2015). A loading-unloading test was carried out with a displacement-force measurement unit (ZTA-500N; EMX-1000N, Imada, Japan). The ends of each specimen were fixed to the clamp of 5 mm. The loading-unloading cycle was repeated 3 times at a speed of 25 mm/min (Henderson et al., 2015). The loading distance was 1.5-6.0 mm depending on the stiffness of the specimen in the linear region. In each trial, the displacement (mm) and load (N) of the tissue were calculated using a software (Force Recorder Professional, Imada, Japan) on a personal computer operating at 1000 Hz. Since the first loading-unloading cycle was substantially deviated from other cycles (the slopes of the regression line between displacement and load relationship were 17.5-25.5% lower compared with the second and third cycles) and considered as preconditioning (Fig. 2-4b), the second and third cycles were analyzed (Bennett et al., 1986). The stiffness, Young's modulus, and hysteresis were calculated from the relationship between the displacement and load of the specimen, in order to compare the mechanical properties of the fascia lata among regions and tensile directions. At each parameter, the measurement values from the second and third loading-unloading cycles were averaged and used as the representative value.

Stiffness

The displacement-load relationship of the loading path in each cycle was divided into the toe region in which the change in tension with respect to displacement was nonlinear, and the linear region in which the elongation and tension changes were proportional (Fig. 2-4c). The point where the residual of the regression line from the top of the loading path sizably exceeded 0 was defined as the transition point of the two regions. The stiffness (N/mm) of the specimen was calculated for the linear region (Mogi et al., 2013).

Young's modulus

Stress (N/mm2) was calculated by dividing the load by the cross-sectional area (average thickness x width) of the specimen. Also, nominal strain (%) was calculated as the elongation of the specimen divided by its initial grip-to-grip length (Stecco et al., 2014). The slope of the regression line in the linear region of the stress-strain relationship was calculated as the Young's modulus of the specimen (Fig. 2-4d).

Hysteresis

To investigate the viscoelastic property of the tissue, the mechanical hysteresis (%) was calculated from the stress-strain relationship (Maganaris and Paul, 2000) (Fig. 2-4e). The energy required to stretch the tissue (WS) and the energy released by the shortening of the tissue (WR) were calculated by integrating numerically the function of displacement upon loading and unloading, respectively. The mechanical hysteresis WH in the loading-unloading cycle was calculated as 100 (WS - WR) / WS (Maganaris and Paul, 2000).

2.2.4. Statistical Analysis

Results were presented as means and standard deviations (S.D.). All the analyses were performed with a statistical software (IBM SPSS Statistics 23, IBM, Armonk, NY, USA). A one-way analysis of variance (ANOVA) with repeated measures was used to compare the relative changes in thickness of the tissues among the four sites (anterior, lateral, medial, posterior) of the thigh. Proportions of the fiber's directions for each site were compared with a one-way ANOVA with repeated measures. A two-way ANOVA was conducted to analyze the effects of loading direction (longitudinal, transverse) and site (anterior, lateral, medial, posterior) on the stiffness, Young's modulus, and hysteresis values. The ANOVAs were followed by post-hoc tests with Bonferroni correction and paired t-tests. To examine the gender differences, two-way ANOVAs with repeated measures were performed for each parameter (gender and site for the thickness, stiffness, Young's modulus, hysteresis; gender and fiber direction for the proportion of fiber's directions), followed by post-hoc tests with a Bonferroni correction and independent *t*-tests. The

significance level was set at $p < 0.05$.

2.3. Results

2.3.1. Morphological properties

Thickness

The specimens from the lateral site (0.8 ± 0.15 mm) of the fascia lata were 3-4 times thicker compared to the other sites (Fig. 2-5a). The anterior site (0.28 ± 0.05 mm) of the fascia lata was significantly thicker than that of the medial site (0.19 ± 0.04 mm). There were no significant gender differences in the thickness at any of the sites (Table 2-1).

Distribution of fiber directions

The proportion of the longitudinally directed fibers ($28.0 \pm 2.8\%$) was slightly but significantly higher than the fibers running in other directions at the anterior site (Fig. 2-5b). At the lateral site, $32.3 \pm 2.6\%$ of the fibers were running in the longitudinal direction which was about 1.5 times higher than those of other directions (19.5-27.1%). The posterior-superior to anterior-inferior (P/A)- diagonally directed fibers were significantly higher in proportion compared with the anterior-superior to posterior-inferior (A/P)- diagonally and transversely directed fibers. The percentage of the transversely directed fibers was significantly higher than that of the P/A- diagonally directed fibers. At the medial site, the proportion of the fibers running in the longitudinal direction was significantly higher than those of the other directions. Females had about 1.3 times higher proportion of transversely directed collagen fibers than males (Table 2-1). The percentage of the lateral-superior to medial-inferior (L/M)- diagonally directed fibers at the posterior site was significantly lower than those of other directions (posterior, $20.3 \pm 1.2\%$; others, 24.5-28.8%). The transversely directed fibers showed significantly higher proportion than the medial-superior to lateral-inferior (M/L)- diagonally directed fibers.

2.3.2. Mechanical properties

Stiffness

The two-way ANOVA showed a significant interaction between loading direction and

site of the specimens. The stiffness of the fascia lata when applying a load in the longitudinal direction was up to 100 times higher than that in the transverse direction at every site (Fig. 2-6a). In the longitudinal direction, the specimens taken from the lateral site (282.7 ± 54.2 N/mm) were significantly stiffer than those from the other sites (19.8-84.2 N/mm). At the anterior site, the fascia lata showed significantly higher stiffness than those from the medial and posterior sites. The stiffness of the specimens from the posterior site was significantly higher than those of the medial site. When applying a load in the transverse direction, the stiffness of the fascia lata from the lateral site (2.8 ± 1.8 N/mm) was at least 3-fold lower compared to the other sites (7.8-15.5 N/mm). The specimens taken from the anterior site were significantly stiffer than the specimens from medial site. At the medial site, the Young's modulus of the females' fascia lata was higher in the longitudinal direction and lower in the transverse direction compared with that of males (Table 2).

Young's modulus

There was a significant interaction between loading directions and sites. The Young's modulus was 2-90 times higher when applying a load in the longitudinal than the transverse direction at every site (Fig. 2-6b). The specimens taken from the lateral site (275.9 ± 83.2 MPa) showed significantly higher Young's modulus in the longitudinal direction than those from the medial (71.6 ± 31.7 MPa) and posterior sites (107.8 ± 63.5 MPa). The Young's modulus of the specimens from the anterior site was significantly higher than those of the medial and posterior sites. In contrast, in the transverse direction, the Young's modulus of the specimens from the lateral site (3.2 ± 2.3 MPa) was about 10 times lower than those from other sites (31.9-41.9 MPa). The Young's modulus of the females' fascia lata at the middle site was higher in the longitudinal direction and lower in the transverse direction compared with that of males (Table 2).

Hysteresis

The two-way ANOVA revealed a significant interaction between loading directions and sites. There was no significant difference in the hysteresis between the loading directions at any sites (Fig. 2-6c). The specimens taken from the lateral site (longitudinal: $33.3 \pm 6.2\%$, transverse:

34.1 ± 5.6%) showed significantly higher hysteresis compared with those of the other sites (20.0-28.0%) both in the longitudinal and transverse directions. Neither direction showed a significant gender difference in hysteresis (Table 2-2).

2.4. Discussion

We measured morphological and mechanical properties of the fascia lata taken from different sites of human cadavers, and demonstrated that the fascia lata showed varied morphological and mechanical properties among the sites on the thigh, which clearly indicates that this tissue is anisotropic. Furthermore, this is the first report that found gender-specific differences in morphological as well as mechanical properties of the fascia lata, the degree of which showed site-specificity.

The morphological characteristics of human soft tissues (skeletal muscles, adipose, and tendinous tissues) have been investigated *in vivo*, by using ultrasonography and magnetic resonance imaging (Maruyama et al, 1991; Kawakami, 2012; Ema et al., 2015). There have also been attempts recently to evaluate mechanical properties of those tissues *in vivo*, by using ultrasound elastography (Xu et al., 2016; Ryu and Jeong, 2017). However, it is still difficult to distinguish between deep fascia and other tissues, and *in vivo* observation of fascial fiber's orientation is impossible at present. Therefore, we carried out a cadaveric study to measure the morphological and mechanical properties of the fascia lata.

The fascia lata at the lateral site was thicker compared to other sites, a similar finding to a previous anatomical and hystological observation that compared the thickness of the fascia lata at the lateral and medial sites (Benjamin, 2009). We also found that the longitudinally directed fibers were the highest in proportion at the lateral site. The concept of epimuscular myofascial force transmission would help us explain why such site-dependent differences of the fascia lata have been shown. The iliotibial tract comprises the lateral site of the fascia lata without any boundary in between and reinforces the lateral side of the thigh (Terry et al., 1986; Evans, 1979; Stecco et al., 2013). Since the lateral site of the fascia lata (iliotibial tract) connects to the tensor fascia lata, gluteus maximus, and gluteus medius muscles as the insertion, the greater mechanical load should be imposed on the lateral site of the fascia lata by the activation of these muscles. In

addition, the mechanical load is transmitted to the longitudinal direction of the iliotibial tract due to adduction and abduction of the hip joint in the single leg standing posture (Tateuchi, 2016). Also, Ema et al. (2015) reported that the vastus lateralis has a larger cross-sectional area at the mid-thigh level compared to other thigh muscles. Therefore, it can be considered that the vastus lateralis exerts greater force compared to other thigh muscles. The fascia lata at the lateral site could receive higher load than other sites through the contraction of the quadriceps muscles and/or during postural sway, so the fibers of the fascia lata would become denser and stiffer than other sites in the longitudinal direction. In fact, at the lateral site, the stiffness and Young's modulus of the fascia lata were highest in the longitudinal direction. However, the hysteresis of the fascia lata at the lateral site was highest both in the longitudinal and transverse directions. This finding implies that the lateral portion of the fascia lata in living humans may not be that stiff, because we repeatedly impose mechanical stress in this portion in daily living as described earlier. But the stiffness and Young's modulus were still highest in this portion after taking its hysteresis into consideration, thus the fascia lata at the lateral site would play an important role as the mechanical basis of the whole thigh.

The stiffness and Young's modulus of the fascia lata at the lateral site in the longitudinal direction were about 100 times higher than in the transverse direction. However, the distribution of the transverse fiber directions was at most 30% lower than the longitudinal fiber directions. In addition, though the large site-dependent differences on the stiffness and Young's modulus were also observed between the lateral and other sites, the proportion of fiber directions showed smaller differences between sites. These results suggest that the differences in the density and/or type of the collagen fibers in addition to the distributions of the fiber directions cause the anisotropic and site-dependent elastic properties of the fascia lata. Further histological studies will clarify the differences between the densities or types of the deep fascia at the different sites of the thigh.

At the medial site, the distributions of the fiber direction and the elastic properties of the fascia lata showed gender-dependent differences. The proportion of the longitudinally directed fiber was higher in males than in females, and the relative amount of the transversely directed fibers was higher in females compared with males. The stiffness and the Young's modulus of females' fascia lata were higher than those of males in the transverse direction, but lower in the

longitudinal direction. These results could explain that the elastic properties of the fascia lata at the medial site are determined by the distribution of the fiber directions composing this tissue. The proportion of females' adipose tissue is higher than that of males, especially at the medial thigh (Maruyama et al., 1991). Besides, females' quadriceps angle is larger than that of males (Horton and Hall, 1989), and those who have the valgus knee possess larger vastus lateralis than those with the normal and varum knee (Sogabe et al., 2009). These factors may explain the gender differences of the morphological and elastic properties of the fascia lata, which warrants further studies.

It has been reported that the thickness of the deep fascia of the fetus was about 0.2 mm (Blasi et al., 2015) and that of the adult was about 0.9 mm (Stecco et al.,2008, Stecco et al., 2009). These studies suggest that the morphological properties of the deep fascia change with growth. In addition, injuries and pathologies could result from the site-differences of the deep fascia's properties. For example, iliotibial band syndrome is common injury in runners and causes lateral knee pain. It had been considered that the repetitive impingement of the iliotibial band against the lateral femoral epicondyle is one of the reason of producing this kind of pain (Orchard et al., 1996). The higher distribution of the longitudinally directed fibers and higher stiffness of the lateral fascia lata were demonstrated in this study. These strong structures of the fascia lata at the lateral site may contribute to the transmission of the high forces produced by the underlying and connecting muscles and could be the reason why higher mechanical stress is applied and injuries are frequently observed at the lateral thigh. Besides, the gracilis and semitendinosus of the children with cerebral palsy who show limited range of motion demonstrated different muscle force-length characteristics depending on the activation strategy (simultaneously vs. separately) (Ateş et al., 2013, 2014, 2016). The higher distribution of the transversely directed fibers in the posterior site, compared with the anterior and lateral site, could contribute to produce such inter-muscular interaction through myofascial connections. Therefore, it is possible that the mechanical properties of the fascia lata change due to aging and these changes may be related to pathological muscle wasting. Further studies are warranted to investigate these issues.

Although this study has quantitatively shown the site- and gender- differences of the fascia lata for the first time, there are some limitations. In this study, we used specimens from

formalin-fixed cadavers. Several studies which focused on the mechanical properties of the deep fascia used frozen or fresh cadavers (Stecco et al., 2014; Henderson et al., 2015), so it is possible that the mechanical tests would have produced different values if we have used other fixation methods. In fact, the values of loading slope and load to failure of the rabbit ligament fixed by the formaldehyde and freezing were lower than the fresh ligament which taken immediately after death (Viidik and Lewin, 1966; Woo et al., 1986). Although the fixation method used in this study may have influenced the properties of the deep fascia, our findings of the site- and gender-specificity of the morphological and mechanical properties of the fascia lata would have been observed regardless of the applied fixation method. In addition, future development of the measurement methods to quantify the morphological and mechanical properties of the deep fascia *in vivo* may reveal the functional roles of the deep fascia during exercise. Such knowledge may further lead to the development of effective interventions (e.g., physical training, manual therapy, and supporting body garments) to optimize the functions of the deep fascia associated with the contractions of the underlying muscles during exercise and sport.

2.5. Conclusion

Our study revealed that the fascia lata at the lateral site was thicker and had higher distribution of the longitudinally directed fibers compared with those of other sites. Also, we demonstrated that the elastic properties in the longitudinal direction were higher at the lateral than other sites. At the medial site of the fascia lata, gender specific differences of the distribution of the fiber directions and elastic properties were observed. Site- and gender-dependence of the morphological as well as mechanical properties of the fascia lata may have resulted from different morphology and mechanics of underlying muscles.
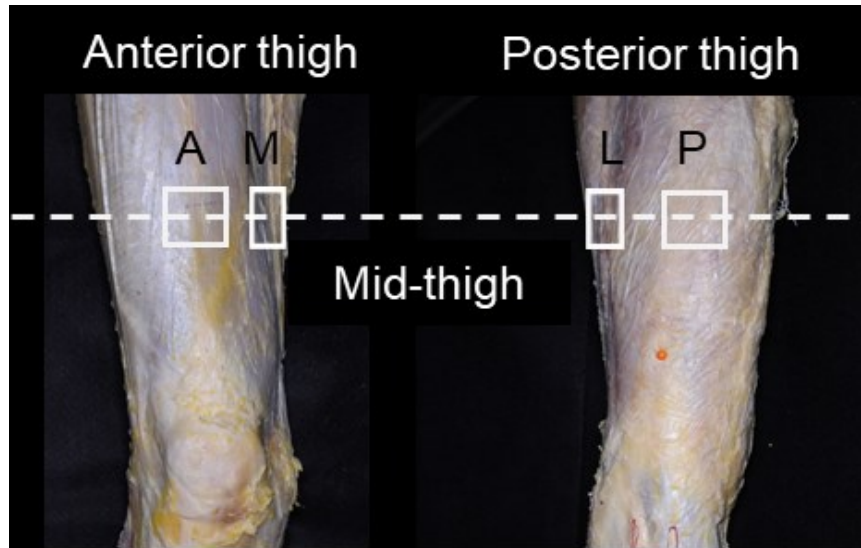
Fig. 2-1.

Pictures showing the anterior and posterior aspects of the thigh of a cadaver with the collected sites of the specimens of the fascia lata. (A: anterior, M: medial, L: lateral, P: posterior)
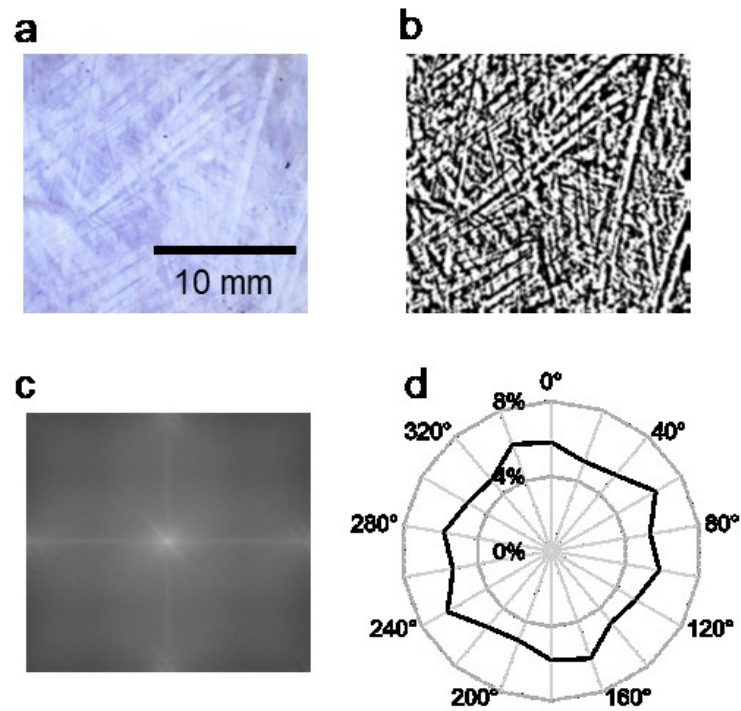
Fig. 2-2.

(a) Original and (b) binarized image of the fascial specimen. The results of (c) fast Fourier transformation and (d) distribution of fibers' directions are also shown.
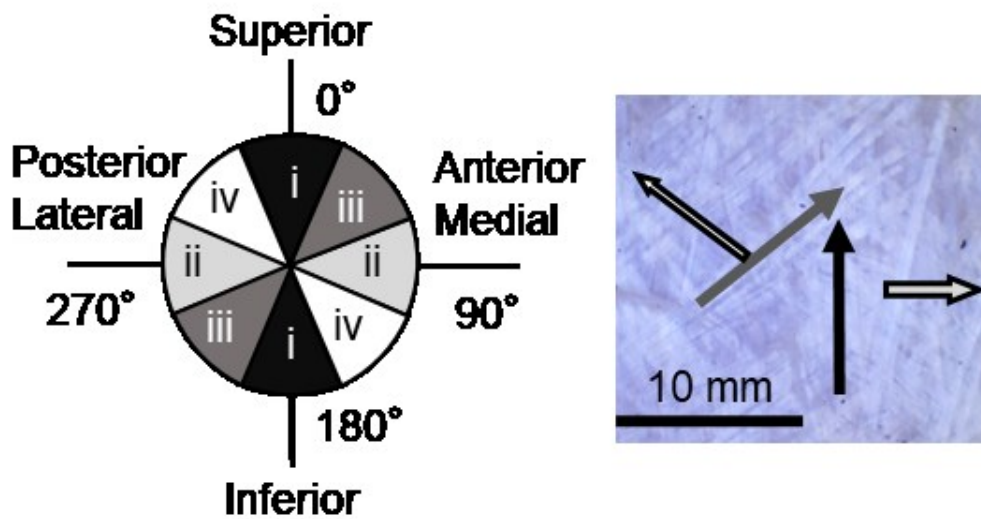
Fig. 2-3.

(a) Classification of the fibers' orientations and (b) typical image of the fascia lata. i: longitudinal (inferior to superior), ii: transverse (anterior to posterior or medial to lateral), iii: M/L- or A/P- diagonal (medial-superior to lateral-inferior or anterior-superior to posterior-inferior), iv: L/M- or P/A- diagonal (lateral-superior to medial-inferior or posterior-superior to anterior-inferior)
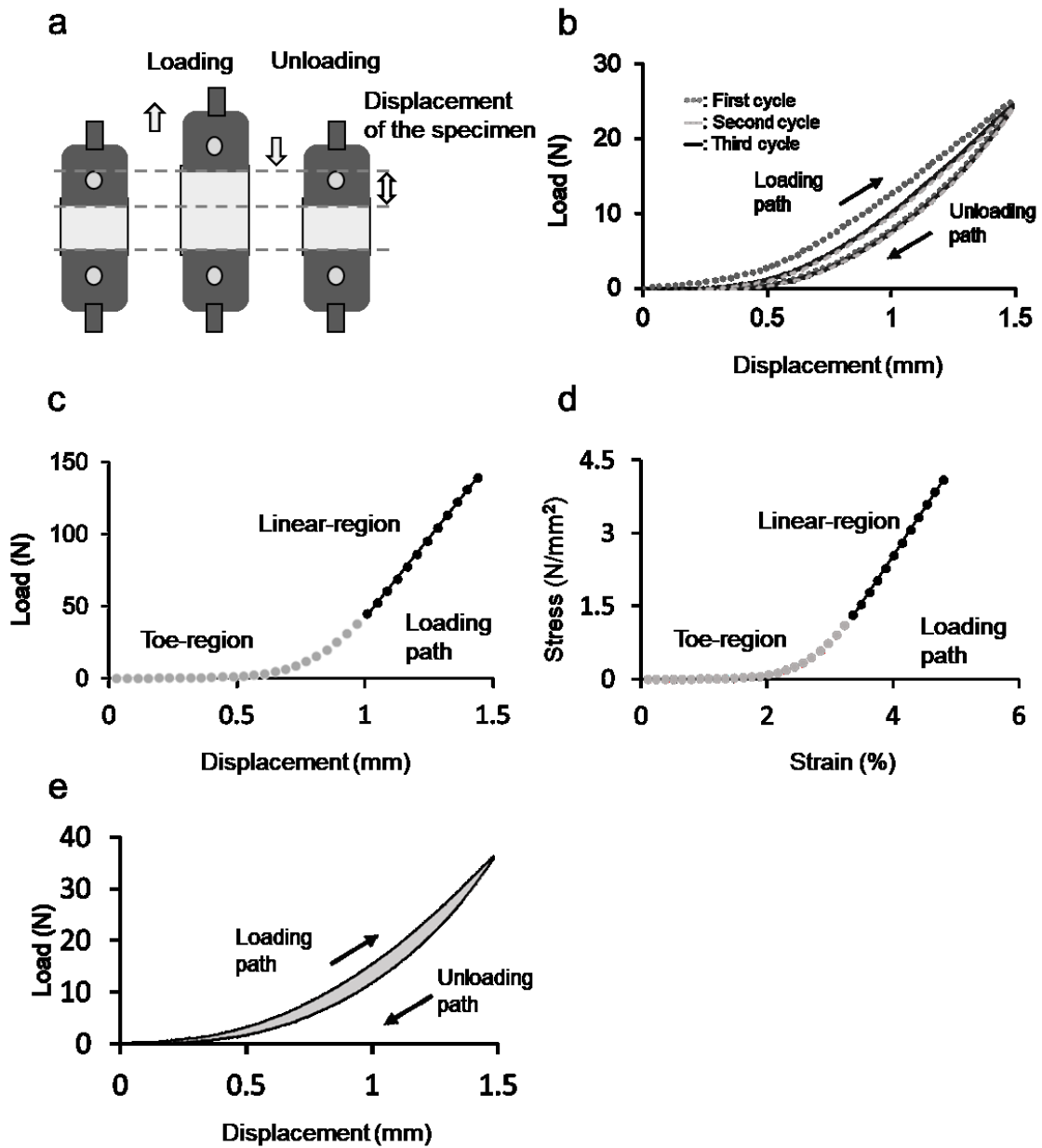
Fig. 2-4.

Mechanical tests for the fascia lata: (a) loading-unloading cycles (b) with the typical results of (c) stiffness, (d) Young's modulus, and (e) hysteresis loop.
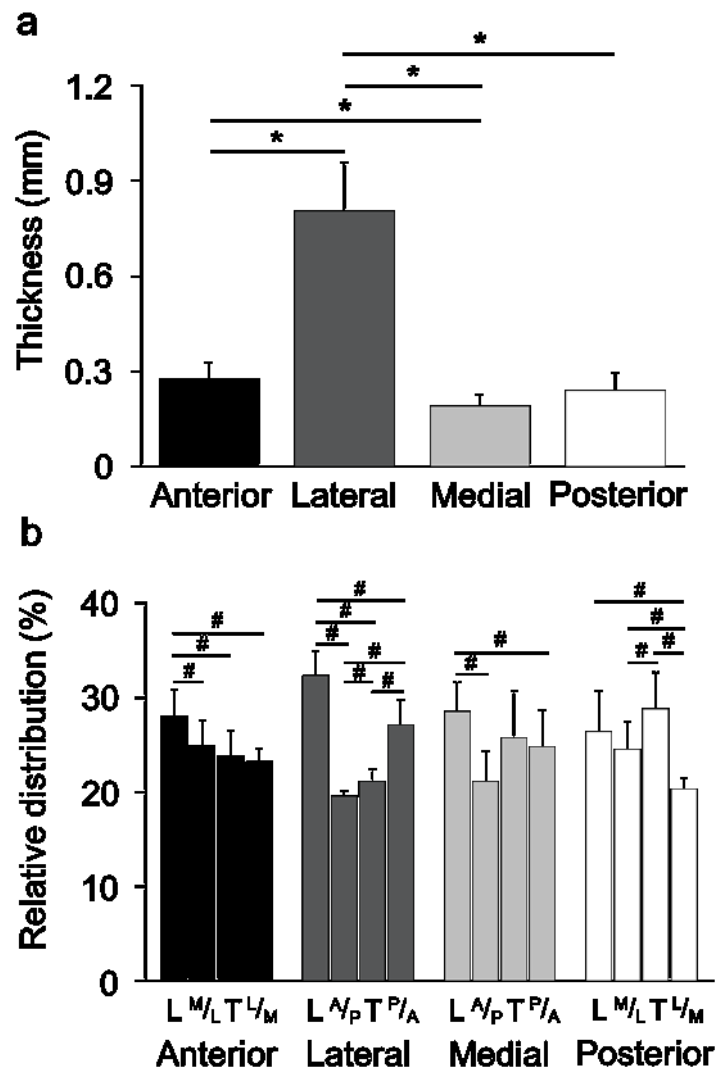
Fig. 2-5.

(a) Thickness and (b) relative distribution of the fibers' orientations of the fascia lata at each site are shown in this figure. Values are means ± S.D. (N = 17). (L: longitudinal, $^M/_L$: M/L- diagonal, $^A/_P$: A/P- diagonal, T: transverse, $^L/_M$: L/M- diagonal, $^P/_A$: P/A- diagonal, *: site-dependent difference, $p < 0.05$, #: difference between each direction, $p < 0.05$)
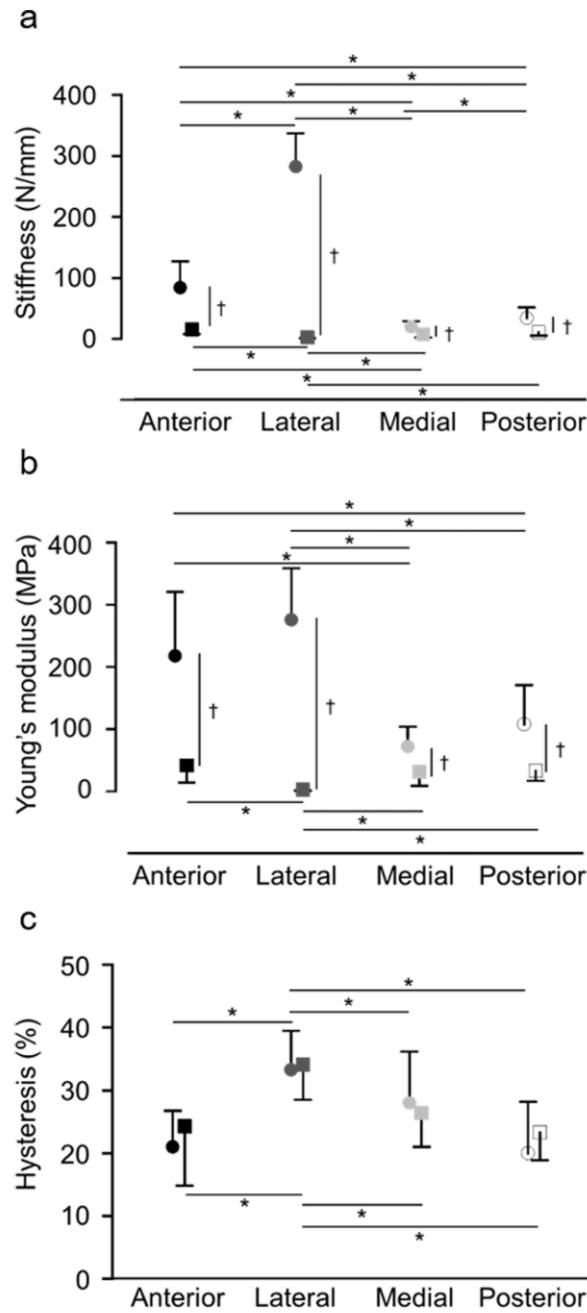
Fig. 2-6.

Figure showing the (a) stiffness, (b) Young's modulus, and (c) hysteresis of the fascia lata taken from each site. Values are means ± S.D. (N = 17). (●: longitudinal direction, ■: transverse direction, *: site-dependent differences, $p < 0.05$, †: direction-dependent differences, $p < 0.05$)

Table 2-1

Morphological properties of the fascia lata of males and females (means ± S.D.).

		Sites							
		Anterior		Lateral		Medial		Posterior	
		Male	Female	Male	Female	Male	Female	Male	Female
Thickness (mm)		0.31 ± 0.04	0.24 ± 0.03	0.78 ± 0.17	0.84 ± 0.13	0.2 ± 0.05	0.18 ± 0.01	0.23 ± 0.06	0.25 ± 0.06
Distribution of fiber directions (%)	Longitudinal	28.5 ± 2.4	27.6 ± 3.3	31.8 ± 2.1	32.8 ± 3.0	30.0 ± 2.1*	27.0 ± 3.3	27.5 ± 2.8	25.2 ± 5.4
	Positively diagonal	26.1 ± 2.9	23.8 ± 2.0	19.4 ± 0.6	19.7 ± 0.6	22.1 ± 3.9	20.0 ± 2.1	25.1 ± 2.8	23.8 ± 3.0
	Transverse	22.6 ± 2.1	25 ± 2.7	21.1 ± 1.6	21.0 ± 1.0	22.5 ± 2.7*	28.9 ± 4.6	27.4 ± 2.9	30.2 ± 4.5
	Negatively diagonal	22.8 ± 1.7	23.6 ± 1.0	27.7 ± 1.7	26.5 ± 3.2	25.4 ± 4.9	24.2 ± 2.7	20.0 ± 1.0	20.7 ± 1.5

*: Male vs. Female with post-hock test, $p < 0.05$; N = 17.

Table 2-2

Mechanical properties of the fascia lata of males and females (means ± S.D.).

		Sites							
		Anterior		Lateral		Medial		Posterior	
		Male	Female	Male	Female	Male	Female	Male	Female
Stiffness (N/mm)	Longitudinal †	109.6 ± 40.9	55.6 ± 24.3	279.0 ± 61.1	286.9 ± 49.3	24.1 ± 9.1	14.9 ± 6.5	39.7 ± 18.8	27.1 ± 15.7
	Transverse	13.3 ± 6.4	17.8 ± 7.9	2.6 ± 2.1	3.2 ± 1.4	4.8 ± 2.5*	11.1 ± 5.7	12.6 ± 4.0	7.7 ± 4.8
Young's modulus (MPa)	Longitudinal †	264.3 ± 90.3	166.3 ± 94.7	289.9 ± 109.1	260.2 ± 41.3	81.4 ± 36.1	60.6 ± 23.5	135.2 ± 71.2	76.9 ± 36.7
	Transverse	33.2 ± 16.5	54.1 ± 34.1	2.8 ± 2.4	3.6 ± 2.2	20.0 ± 15.5*	45.4 ± 22.6	41.9 ± 13.2	22.2 ± 12.6
Hysteresis (%)	Longitudinal	25.2 ± 5.4	24.5 ± 8.1	46.2 ± 8.0	41.4 ± 5.8	36.6 ± 23.2	26.0 ± 3.2	24.3 ± 10.1	22.8 ± 7.2
	Transverse	27.2 ± 11.5	25.4 ± 18.3	35.6 ± 4.2	40.1 ± 4.8	32.6 ± 4.4	26.7 ± 4.5	26.1 ± 3.9	28.6 ± 5.6

*: Male vs. Female with post-hock test, $p < 0.05$, †: main effect of gender, $p < 0.05$; N =17.

CHAPTER 3

Dependence of muscle and deep fascia stiffness on the contraction levels of the quadriceps: an *in vivo* supersonic shear-imaging study

3.1. Introduction

In chapter 2, the dependence of the morphological and mechanical properties of the deep fascia on the sites and genders was obserbed. However, that study was subjected to the human cadavers so that the mechanical interactions between muscles and deep fascia during motor performance still remains to be determined. In this chapter, the elastic properties of the fascia lata and underlying muscles were measured using ultrasound shear wave elastography (SWE) *in vivo*. The aim was to investigate the inter-dependence in mechanical properties between fascia lata and neighboring muscles as well as site- and direction-differences, at different contraction intensities of the isometric knee extension.

3.2. Material and methods

3.2.1. Participants

The present study was approved by the local ethical committee. Fourteen healthy males (age, 26 ± 4 years: height, 171.5 ± 6.2 cm: body mass 65.5 ± 11.0 kg; means $\pm$ SDs) gave their written informed consent before participating in this study.

3.2.2. Experimental design

The participants seated on an isometric dynamometer (VTE-002R, VINE, Japan). The locations of the ultrasound transducer were determined from B-mode images of the ultrasound (Aixplorer version 6.4, Supersonic Imagine, Aix-en-Provence, France), and markers were applied on the skin using a waterproof pen for the rectus femoris (RF) and vastus lateralis (VL) muscles in the longitudinal and transverse directions (Fig. 3-1). The shear wave velocity (SWV) of the muscles and fascia lata in the passive condition was measured twice at each site and direction in a random order using ultrasound shear wave elastography. The participant was orally instructed to stay completely relaxed and without any muscle contraction during the passive condition. After

five sub-maximal contractions as a standardized warm-up, each participant performed the maximal voluntary contraction (MVC) of isometric knee extension for 3 s. More than two trials were performed if peak torques were substantially different (> 10%). Following the MVC trials, the participants performed sub-maximal isometric knee extensions for 7 s at 20, 40, and 60% of the highest values of the MVC in a random order for two sets. The SWV was measured at two sites and two directions during contractions separately in a random order. More than 1 min of rest was taken between contractions. During contraction and at rest, knee extension torque and surface electromyography (EMG) from RF and VL were recorded.

3.2.3. Measurements

Shear wave elastography

The SWV of the RF and VL muscle bellies (midpoint of the greater trochanter and lateral condyle of the femur) on the right leg and fascia lata over these muscles was measured using an Aixplorer ultrasonic scanner with a linear array ultrasound transducer (L15–4, Supersonic Imagine, Aix-en-Provence, France) in the supersonic shear imaging (SSI) mode. We coupled the ultrasound transducer to the skin surface using an acoustic stand-off (Enraf-Nonius, France) (for fascia lata) and ultrasound gel (for muscle bellies), ensuring minimum pressure between the transducer and skin. Maps of the SWV were obtained at 12 Hz with a spatial resolution of 1 x 1 mm. RF and VL muscles and the fascia lata over these muscles were tested in the longitudinal (parallel to the muscle fascicle) and transverse (orthogonal to the longitudinal) probe directions (Fig. 3-2). The region of interest (ROI) for the muscles and fascia lata was set manually. In this study, the SWE device was operated by an experienced single examiner.

Knee extension torque

The participants were seated on the dynamometer, with 80˚ and 70˚ of hip and knee joint angles, respectively (0˚ = full extension of hip and knee). The trunk of the participant was secured to the backrest of the dynamometer to restrict any upper body movement. The pad on the actuator arm of the dynamometer was securely fastened to the participant's right leg just above the medial malleolus. The torque data were amplified by a strain amplifier (DPM-711B, Kyowa, Japan). The

data were recorded through an analogue to digital converter (Power Lab, AD Instruments, Australia) in a personal computer at a sampling frequency of 1,000 Hz after 10 Hz low-pass filtering.

Surface electromyogram

Surface electromyogram (EMG) was recorded through the test using a wireless EMG system (Trigno, Delsys, USA). After preparation of the skin (shaving, abrading, and cleansing with ethanol), EMG electrodes were placed over the belly of RF and VL muscles just above the location of the ultrasound transducer and parallel to the orientation of the muscle fibers. EMG signals were amplified and recorded through the analog-digital converter in a computer at a sampling frequency of 1000 Hz after bandpass-filtering (20-450 Hz).

3.2.4. Data analysis

Knee extension torque was normalized to the value during MVC. The SWV of muscles and fascia lata was measured by the ultrasound device. The muscle bellies and boundaries of the fascia lata were chosen manually as the ROI in the shear wave map, avoiding hypoechoic and saturated regions (Fig. 3-2). A spatial average value of the SWV over the selected ROI at each image was calculated using the SSI software (Q-BoxTM Trace). Taking into account the mechanical delay of the SWV mapping (Sasaki et al., 2014), five images (every one second from 2 to 6 within 7 s contraction) in each condition were analyzed and the average value was used as representative of the condition. Average torque and root mean square (RMS) values of EMG over the same time window as of SWV (average value of the 4 seconds) were normalized to MVC (average of 0.5 seconds around the highest torque) (Yoshitake et al., 2014). The slope of the regression line over the relationship between normalized SWV (%SWV; normalized to the value at rest) and normalized RMS (%RMS_{EMG}; normalized to MVC) values at different contraction levels was determined as the degree of stiffness change of each tissue.

3.2.5. Statistics

To examine whether the exerted torque was kept as instructed, one sample t-test was

performed for the torques (normalized to MVC) and target levels (20, 40, 60% MVC). A paired t-test was performed to compare the %RMS$_{EMG}$ values between RF and VL at each contraction level. For the intra-session reliability, the coefficient of variation (CV), standard error of measurement (SEM), and intraclass correlation coefficient (ICC) were calculated. The SWV of the muscles and fascia lata at each site was compared by a two-way analysis of variance (ANOVA) (probe directions x muscle contraction levels) followed by a paired t-test and a one-way ANOVA with Bonferroni corrected post-hoc test. Pearson product-moment correlations were performed to %SWV-%RMS$_{EMG}$ relationships at each site and direction. The slopes of %SWV-%RMS$_{EMG}$ relationships of respective tissues were compared with a two-way ANOVA (sites x probe directions) followed by a paired t-test. To compare the slopes between muscle and fascia lata, a paired t-test was performed. Microsoft Excel (Excel 2016, Microsoft, USA) and SPSS statistical software (SPSS Statistics 24, IBM Corporation, USA) were used to perform these statistics. The significance level was set at $p < 0.05$.

3.3. Results

3.3.1. Shear wave elastography

The CV, SEM, and ICC of SWV values for each tissue, site, probe direction, and contraction level are shown in table 3-1. The ICC of the muscles (0.62-0.99) and fascia lata (0.68-0.99) showed that the SWV was kept "almost perfectly (0.81-1.00)" and "substantially (0.61-0.80)" same in the two cycles of the measurements, except for the fascia lata over VL in the transverse direction at 60% MVC (0.217; "fair") and VL muscle in the transverse direction at 20, 40, and 60% MVC (0.60, 0.57, 0.60, respectively; "moderate") (Landis et al., 1977).

Table 3-2 shows the SWV of the muscles and fascia lata at each site, probe direction, and contraction level. Significant interactions between probe directions and muscle contraction levels were found at each site of fascia lata and muscle both for RF and VL ($p < 0.01$). In both directions, the SWV of the fascia lata increased with higher contraction levels. In every contraction level, the fascia lata over VL showed significantly higher SWV than that of RF ($p < 0.01$). At all levels of contraction, the SWV of the fascia lata in the longitudinal direction was significantly higher than that of the transverse direction ($p < 0.01$). For both muscles, the SWV in

the longitudinal direction was lower than that of the transverse direction at rest ($p < 0.01$), but was higher during contraction ($p < 0.01$) except for that of RF at 20% MVC ($p = 0.09$). The SWV of the muscles in the longitudinal direction increased with higher levels of contraction ($p < 0.05$). In the transverse direction, the SWV of the muscles was higher at 20, 40, 60% MVC than at rest ($p < 0.05$).

3.3.2. Slope of the relationship between %SWV and %RMS$_{EMG}$

%SWV and %RMS$_{EMG}$ of both the fascia lata and muscles showed significant and positive correlation at every site and direction ($p < 0.05$) (Fig. 3-3). A significant main effect of the direction was shown at each site of the fascia lata and muscles. The slopes of those changes of the fascia lata and muscles were higher in the longitudinal than transverse direction ($p < 0.01$) (Table 3).

3.3.3. Torque exertion and muscle activation

Average values of the %RMS$_{EMG}$ of each muscle and %SWE of the fascia lata and muscles at each contraction level are shown in Fig. 3-4. Knee extension torques were sustained at $20.8 \pm 1.6\%$, $40.7 \pm 1.9\%$, and $60.8 \pm 1.8\%$MVC, which were not significantly different from the target levels (20, 40, and 60%MVC). Muscle contraction levels were not significantly different between RF and VL except for 20% MVC which showed higher %RMS$_{EMG}$ in VL ($21.7 \pm 5.8\%$) than in RF ($14.8 \pm 4.9\%$).

3.4. Discussion

The present study showed dependence of the fascia lata and quadriceps muscles stiffness on the level of knee extension torque exertion. To the best of our knowledge, this is the first study that delineated deep fascia's mechanical behavior associated with underlying muscle contractions. The stiffness of RF and VL muscle bellies in the longitudinal direction increased with increasing contraction levels, which is in line with several previous studies (Nordez and Hug, 2010; Yoshitake et al., 2014; Ateş et al., 2015). Regardless of the ultrasound probe's direction, the stiffness of RF and VL was similar at rest and during sub-maximal contractions in most cases. In

addition, the slopes of the relationships between %SWV and %RMS$_{EMG}$, i.e., the degrees of stiffening, of RF and VL, were almost identical for longitudinal and transverse directions. No studies have ever examined changes in the stiffness of the quadriceps muscles during contraction, and the present study indicates that RF and VL muscles become stiffer with similar degrees under the same intensity of isometric contraction in the present knee and hip joint configuration.

Regarding the fascia lata, the SWV over VL was higher than that over RF at rest and during contraction in both transducer directions. In a human cadaver study, we have found that the fascia lata over VL is thicker and stiffer than that over RF (Otsuka et al., 2018). Such *ex situ* findings suggest that morphological differences (e.g. thickness, collagen fibers direction, and tissue composition) also affect fascia lata stiffness *in vivo*. Interestingly, the degree of stiffening of the fascia lata as a function of contraction intensity was comparable for the two sites. This suggests that the degree of stiffening in the present study is a function predominantly of contraction intensity of the underlying muscles, regardless of the morphological differences in the fascia lata. The degree of stiffening of the fascia lata, however, was lower than that of the muscles especially in the longitudinal direction. Anatomical observation has shown that muscle fibers insert directly into the deep fascia and/or are connected to it via the epimysium (Stecco et al., 2014). Due to such connections, a large amount of the forces, generated by the muscle fibers can be transmitted to the adjacent connective tissues that surround the muscles (Rijkelijkhuizen et al., 2005). It is therefore likely that the fascia lata becomes stiffer according to the passive mechanical stress from underlying muscles' contraction through the myofascial network, and that the relative amounts of stiffness changes are not identical between muscles and fascia lata. Additionally, those connective tissues transmit forces not only serially but also laterally to the neighboring muscles (Maas and Sandercock, 2010). In the present study, knee extension torque was kept at the target level in spite of different muscle contraction levels between RF and VL at 20%MVC, which may affect epimuscular myofascial force transmission between synergist muscles.

Although the SWV of each tissue in the longitudinal direction was lower than that of the transverse direction at rest except for the fascia lata over VL, it became significantly higher during contractions. Our previous study on *ex situ* fascia lata revealed a higher stiffness in longitudinal than in transverse direction (Otsuka et al., 2018). The result of the present study

supports this cadaveric finding and further adds to a notion that the fascia lata becomes stiffer as increasing contraction levels which is prominent in the longitudinal direction compared to the transverse direction. It is generally known that the tendons which are in series with muscles play an important role in elastic energy storage during counter movement exercise (Kawakami et al., 2002). Aponeuroses covering muscle belly can contribute to elastic energy storage and recovery by being stretched in the longitudinal direction and increasing its longitudinal stiffness during contraction (Azizi and Roberts, 2009). In this study, the fascia lata also became stiffer in the longitudinal direction during contraction. This suggests that the fascia lata can act as a spring, contributing to elastic energy storage, myofascial force transmission, and limb stability (Eng et al., 2018; Wilke et al., 2018). The epimuscular myofascial force transmission could occur not only in the direction parallel to muscles but also radially (Findley et al., 2015), and this could be due to the radial expansion of the contracting muscle fibers (Eng et al., 2018). Such a radial expansion may involve lateral stretch and hence stiffening of the fascia lata in the transverse direction. Less stiffness of the fascial tissues in the transverse direction could contribute to maintaining intramuscular pressure (Garfin et al., 1981) and allow for underlying muscle's radial expansion (Eng et al., 2018). It is speculated that such deformations of the fascia lata in both longitudinal and transverse directions match and optimize underlying muscles' contractions, thereby comprising a myofascial functional entity (Fig. 3-5).

We should mention limitations to the present study including our methodology. We found high reliability of the SWE measurements in the longitudinal direction (ICC: 0.618-0.989), but ICC values of SWV were lower in the transverse direction at sub-maximal contraction levels (e.g., ICC: 0.217; fascia lata over VL at 60% MVC). Several SWE studies mentioned about the lower reliability in the transverse probe direction than in the longitudinal direction for tendons (Brum et al., 2014). We found larger differences of the SWV among muscle contraction levels than intra operator differences (SEM) at each contraction level, implying that the measurement error is not so large as to affect data analysis in the present study. However, this should be carefully taken into consideration when one measures the soft tissues in the transverse direction using SWE. In addition, we could only measure up to 60%MVC of the isometric knee extension because of the limit of SWE machine to measure SWV (~16.3 m/s). In our daily life, thigh muscles are

activated by ~20%MVC at most (Kern et al., 2001; Sawai et al., 2006). Thus, the present contraction levels cover a large amount of daily motor tasks and our results indicate that the fascia lata contributes to optimizing underlying muscles functions during daily activities. However, in this study, muscle contraction level of RF and VL was not identical at 20%MVC, which is in line with the previous finding (Alkner et al., 2000). Differences of contraction levels between muscles might be due to difference in size and recruitment patterns of those muscles (Alkner et al., 2000). Besides, we measured the muscle contraction level only from two synergist muscles, although epimuscular myofascial force transmission could also occur between antagonistic muscles and across the joints (Huijing et al., 2007; Cruz-Montecinos et al., 2016). Further studies are warranted to investigate the stiffness changes of the deep fascia at different sites including synergist and antagonist muscles with lower muscle contracrion levels (~20%MVC).

3.5. Conclusion

In conclusion, our study showed that not only the quadriceps muscles but also the fascia lata become stiffer when increasing the level of isometric knee extension torque. There is anisotropy in the elastic properties of the muscles and fascia lata during muscle contractions as well as the way they change as a function of contraction levels. These results further imply that the deformations of the fascia lata in both longitudinal and transverse directions match and optimize underlying muscles' contractions.
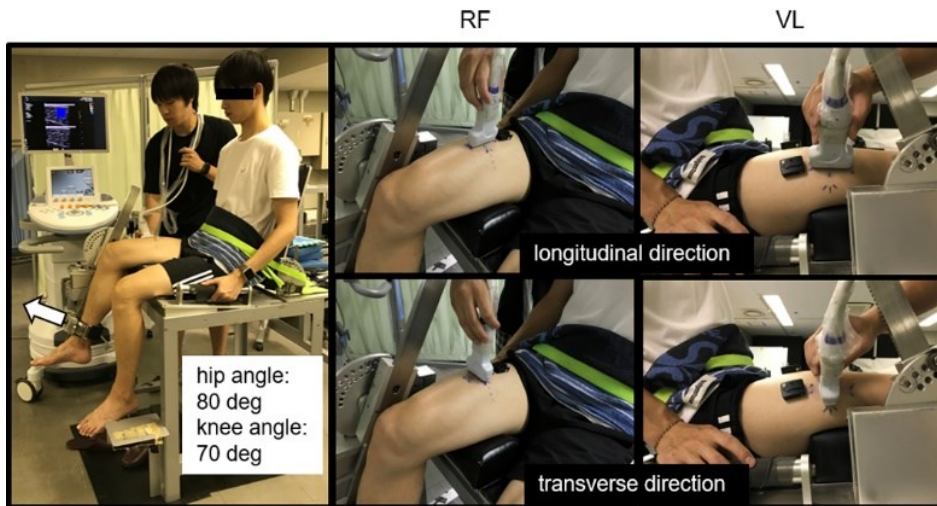
Fig. 3-1.

The posture of the participant during the test and measurement sites of surface electromyography (EMG) and ultrasound shear wave elastography (SWE). The transducer of SWE was placed on the skin over the mid-belly of the rectus femoris (RF) and vastus lateralis (VL) both in longitudinal and transverse directions. The EMG was measured from RF and VL just superior to the SWE transducer for each muscle.
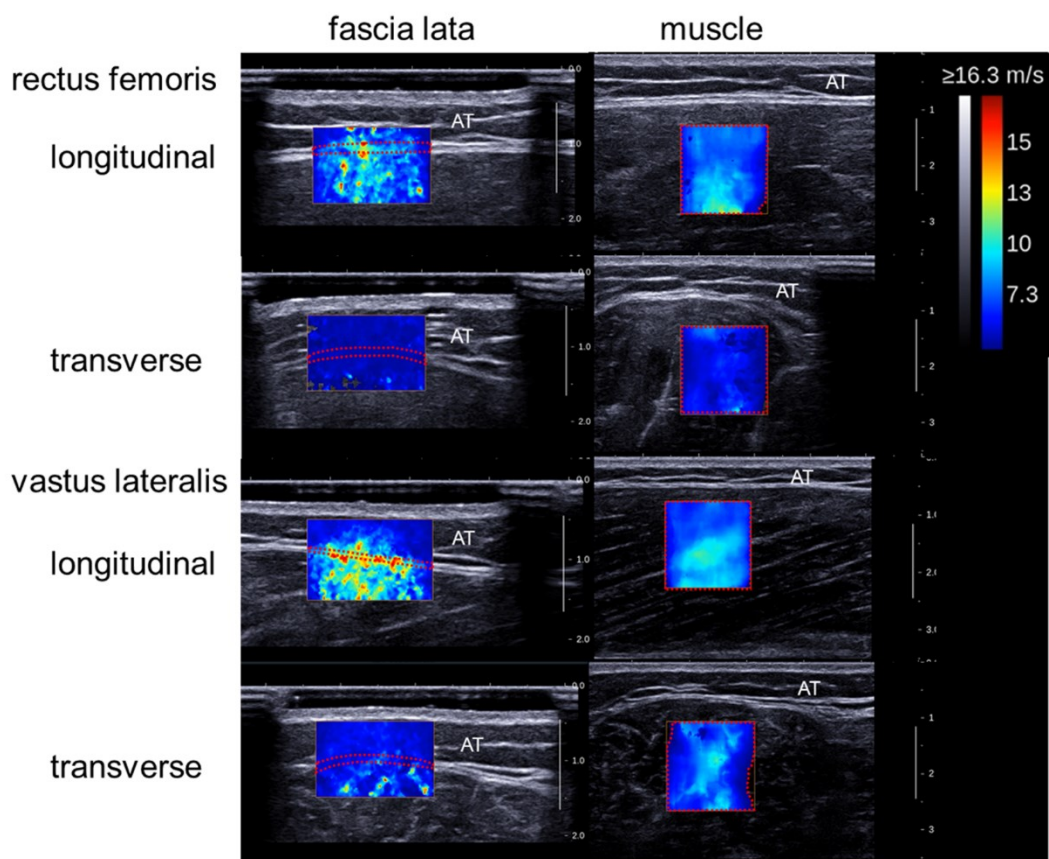
Fig. 3-2.

Typical maps of the shear wave velocity (SWV) and regions of interest (ROIs) of the muscles and fascia lata during sub-maximal contraction in the longitudinal and transverse directions. RF: rectus femoris, VL: vastus lateralis, AT: adipose subcutaneous tissue.

Table 3-1.

Repeatability of SWV measurements from two sets of sub-maximal contractions.

fascia		forces (%MVC)	at rest	20%	40%	60%
RF	longitudinal	CV (%)	3.5	6.1	7.1	6.5
		SEM (m/s)	0.01	0.12	0.14	0.14
		ICC	0.97	0.79	0.85	0.88
	transverse	CV (%)	1.4	7.2	4.9	5.6
		SEM (m/s)	0.004	0.14	0.09	0.15
		ICC	0.99	0.69	0.80	0.68
VL	longitudinal	CV (%)	2.3	6.7	6.4	7.3
		SEM (m/s)	0.01	0.08	0.17	0.39
		ICC	0.99	0.97	0.91	0.70
	transverse	CV (%)	3.3	5.7	5.8	9.1
		SEM (m/s)	0.04	0.12	0.15	0.41
		ICC	0.92	0.78	0.75	0.22

muscle		forces (%MVC)	at rest	20%	40%	60%
RF	longitudinal	CV (%)	3.4	6.0	10.2	6.8
		SEM (m/s)	0.02	0.10	0.37	0.24
		ICC	0.95	0.91	0.62	0.75
	transverse	CV (%)	4.2	8.8	9.3	6.7
		SEM (m/s)	0.04	0.12	0.15	0.41
		ICC	0.95	0.65	0.83	0.83
VL	longitudinal	CV (%)	1.3	3.6	4.6	6.8
		SEM (m/s)	0.01	0.04	0.10	0.23
		ICC	0.86	0.97	0.93	0.85
	transverse	CV (%)	4.0	8.4	9.2	9.0
		SEM (m/s)	0.04	0.25	0.29	0.31
		ICC	0.95	0.60	0.57	0.60

Values show coefficients of variation (CV), standard errors of measurement (SEM), and interclass correlation coefficients (ICC) of shear wave velocity of the rectus femoris (RF) and vastus lateralis (VL) and the fascia lata.

Table 3-2.

The SWV values of the fascia lata and muscle belly at each site and direction.

		shear-wave velocity (m/s)			
		RF		VL	
	contraction level	longitudinal	transverse	longitudinal	transverse
fascia lata	at rest	2.5 ± 0.5 [*20,40,60,†,$]	3.2 ± 0.5 [*40,60,$,#]	4.2 ± 0.8 [*20,40,60,†,#]	3.9 ± 0.5 [*20,40,60]
	20%	4.1 ± 0.6 [*40,60,†,$,#]	3.6 ± 0.3 [*40,60,$,#]	7.5 ± 2.2 [*40,60,†]	4.4 ± 0.5 [*40,60,#]
	40%	5.0 ± 0.8 [*60,†,$,#]	4.1 ± 0.4 [*60,$,#]	8.8 ± 1.7 [*60,†]	4.9 ± 0.6 [*60]
	60%	5.9 ± 1.0 [†,$,#]	4.5 ± 0.4 [$]	9.9 ± 1.2 [†,#]	5.1 ± 0.5
muscle	at rest	2.4 ± 0.3 [*20,40,60,†]	3.6 ± 0.7 [*20,40,60]	2.6 ± 0.3 [*20,40,60,†]	3.7 ± 0.6 [*20,40,60]
	20%	5.2 ± 1.0 [*40,60,$]	4.6 ± 0.6	6.5 ± 1.0 [*40,60,†]	4.8 ± 0.6
	40%	9.1 ± 2.2 [*60,†,$]	4.6 ± 0.8	8.1 ± 1.2 [*60,†]	4.8 ± 0.6
	60%	10.4 ± 3.7 [†]	4.7 ± 0.7	9.1 ± 1.4 [†]	5.2 ± 0.8

Values are means ± SD. *20, *40, *60: vs. 20, 40, 60%, respectively. †: vs. transverse direction. $: vs. vastus lateralis. #: vs. muscle, $p < 0.05$.

Table 3-3.

The slopes of the relationships between %SWV and %RMS$_{EMG}$.

The slope of the relationship between %SWV and %RMS$_{EMG}$	site			
	RF		VL	
	longitudinal	transverse	longitudinal	transverse
fascia lata	$2.6 \pm 1.4^{\dagger,\$}$	0.8 ± 0.6	$2.5 \pm 1.0^{\dagger,\$}$	0.5 ± 0.2
muscle	$4.8 \pm 2.7^{\dagger}$	0.5 ± 0.5	$4.2 \pm 1.0^{\dagger}$	0.7 ± 0.6

Values are means $\pm$ SD. $\dagger$: vs. transverse direction. $\$$: vs. muscle, $p < 0.05$.
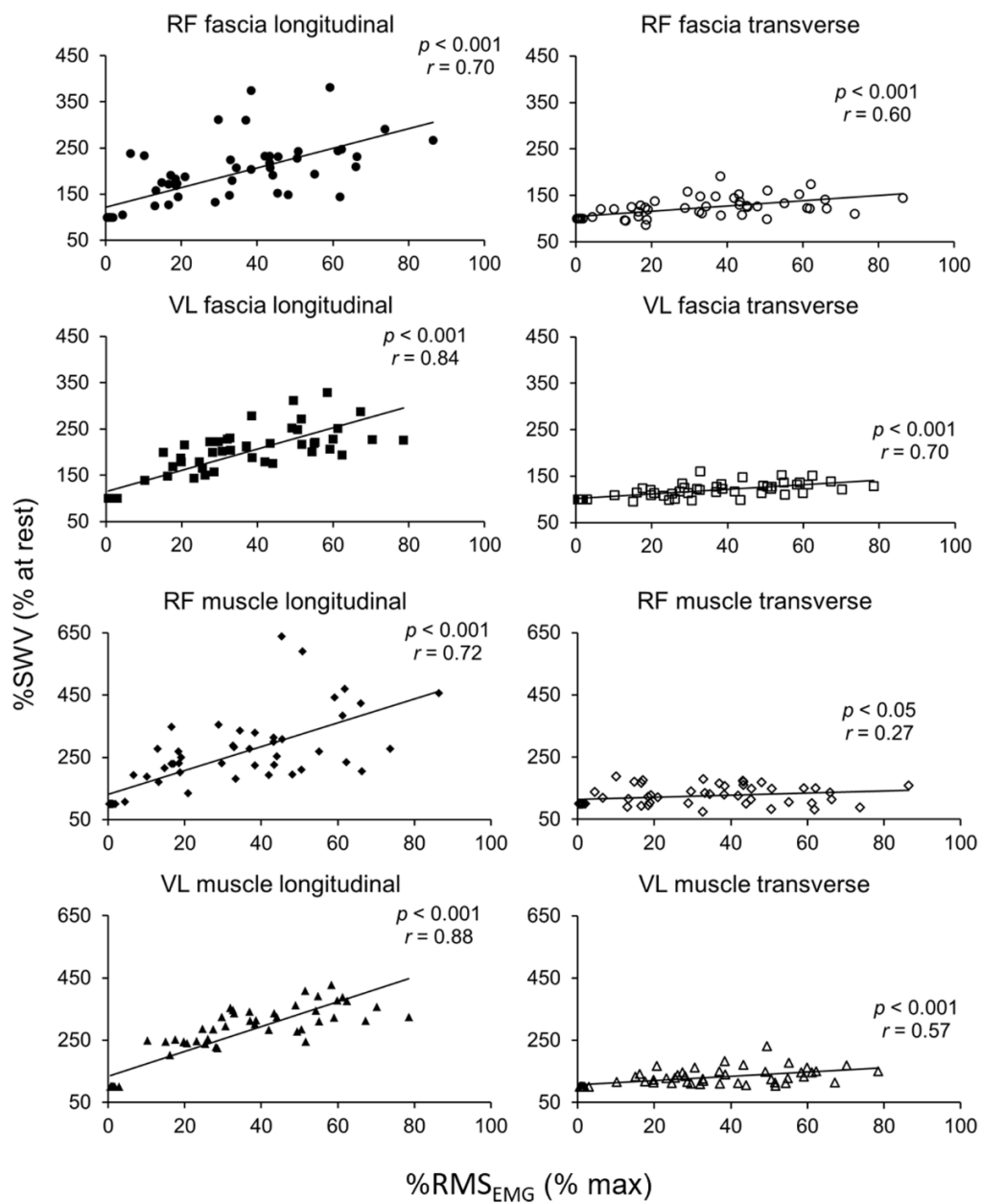
Fig. 3-3.

Relationships between relative values of SWV (%SWV) and EMG RMS (%RMS$_{EMG}$) over and within muscles (fascia lata: RF; circle, VL; square, muscle: RF; diamond, VL; triangle) in the longitudinal (shaded) and transverse (unshaded) directions.

63
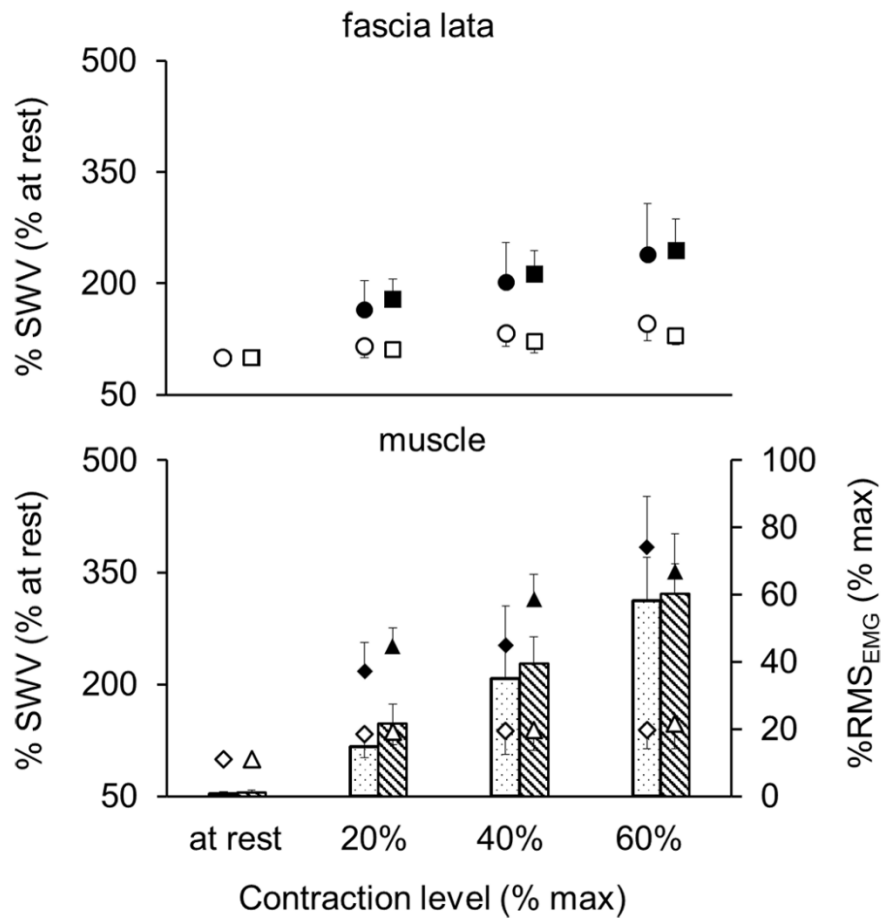
Fig. 3-4.

Average values of %SWV of the fascia lata (RF: circle, VL: square) and muscles (RF: diamond, VL: triangle) in the longitudinal (shaded) and transverse (unshaded) directions at rest and each contraction level. The bar graph shows the %RMS$_{EMG}$ of the muscles (RF: dots, VL: stripe).
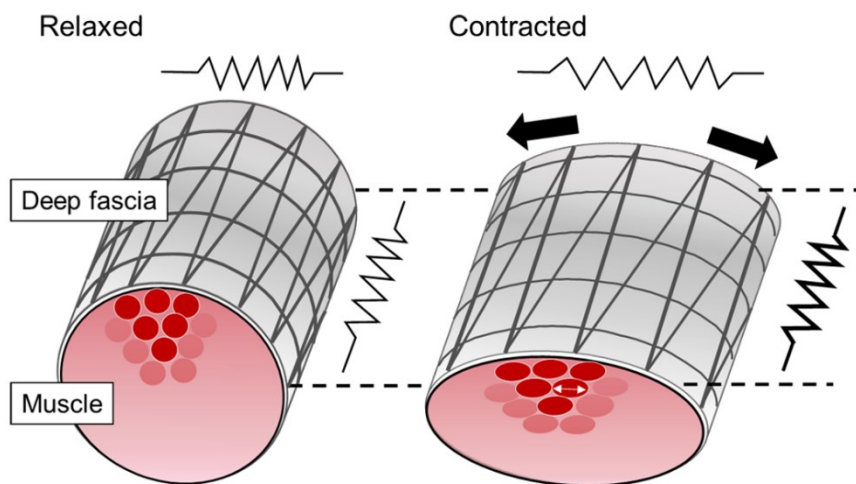
Fig. 3-5.

Schematic illustrations of the changes in fascia lata with muscle contraction. The fascia lata can act as a spring with its elasticity showing anisotropic changes by contraction.

CHAPTER 4

Effect of joint angle configurations on the elastic property of human iliotibial band

4.1. Introduction

From the *ex situ* and *in vivo* study of chapter 2 and chapter 3, outstanding features of the lateral site of the fascia lata (ITB) were observed. ITB may have the potential to assist and coordinate body movements according to its outstanding structures. On the other hand, due to such thick and stiff characteristics, greater mechanical load may concentrate on that part, which could cause ITB related injury (e.g. ITB syndrome). Several studies reported that the ITB syndrome frequently occur near the patella with the knee at 20-30° (Orchard et al., 1996; Noble et al., 1980; Fairclough et al., 2007), but there are limited studies which examined the site-and joint angle-dependent morphological and mechanical properties of ITB in detail. In chapter 4, we aimed to investigate the hypotheses that the morphological and mechanical properties of ITB are site-specific, and change accompanied by the alteration of joint angles.

4.2. Material and Methods

4.2.1. *In vivo* study

Participants

The present *in vivo* study was approved by the local ethical committee at Waseda University. 12 healthy males (age: 26 ± 3 years, height: 174.1 ± 4.3 cm, body mass: 66.7 ± 10.9 kg; means $\pm$ SDs) gave their written informed consent and participated in this study.

Ultrasound measurement

The participants seated on an isokinetic dynamometer (CON-TREX MJ, CMV AG, Switzerland). The trunk of the participant was fixed to the backrest of the dynamometer to avoid any upper body movement. After determination of the locations of the ultrasound transducer from B-mode images of the ultrasound (Aixplorer version 6.4, SuperSonic Imagine, Aix-en-Provence, France), the shear wave velocity (SWV) of ITB was measured using the same ultrasound device with a linear array ultrasound transducer (L15–4, SuperSonic Imagine, Aix-en-Provence, France)

which was placed parallel to the longitudinal directed collagen fibers of ITB. The SWV was measured from five sites of ITB (over the proximal, middle, and distal sites of the vastus lateralis (VL); site 1-3, superior border of the patella; site 4, and between femur and tibia; site 5; Fig.4-1). The SWV of ITB was also studied at nine different joint positions, which were the combinations of knee (0°, 25°, 90°) and hip (0°, 40°, 90°) joint angles (0° being full extension of hip and knee) (Fig.4-2). Two cycles of measurements were conducted to each site and position in a random order. Ankle joint angle was kept at 90° throughout the measurement. The ultrasound transducer was coupled to the skin surface using an acoustic stand-off (Enraf-Nonius, France) and ultrasound gel, ensuring minimum pressure from the transducer to the skin. Maps of the SWV were obtained at 12 Hz with a spatial resolution of 1 x 1 mm. The region of interest (ROI) for ITB was set manually. A single examiner operated the SWE device in this study.

Calculation of the SWV

The SWV of ITB was measured by the ultrasound device. The boundaries of ITB were chosen manually as the ROI in the shear wave map (Fig.4-3). A spatial average value of SWV over the selected ROI at each image was calculated using the software installed in the device (Q-Box^{TM} Trace). An average value of the SWV over the ROI was calculated from each image. Three images (every one second) from each site and position were analyzed and the average value of two measurement cycles was determined as the representative value.

4.2.2. Cadaveric study

Specimen preparation

We investigated ITB specimens taken from five different sites of formalin-fixed human cadavers (12 male right legs, age: 69-93 years). The experimental design of this cadaveric study was approved by the ethics committee at Aichi Medical University. Specimens of ITB were harvested from five sites corresponding to those of *in vivo* study (Fig.4-3). Specimens were 40 x 20 mm (over the proximal, middle and distal sites of VL) and 30 x 10 mm (superior border of the patella, and between femur and tibia) in the longitudinal and transverse directions depending on the width and length of ITB at each region. The direction from the end of tensor fascia lata to the

Gardy's tubercle of the tibia was defined as the longitudinal direction and the orthogonal direction to it was as the transverse direction. Adipose and loose connective tissues were manually removed from the specimens using tweezers taking great care of avoiding any damage to the specimen. After collection, the specimens were stored in a 20% formaldehyde solution (same solution for embalming) at room temperature.

Tensile test

The thickness of ITB was measured with a digital caliper (LIXIL VIVA, Japan) (Kumar et al, 2011; Hwang et al., 2012). Three different points (proximal, middle, and distal parts) of each specimen were randomly selected and the average value of two measurement cycles was calculated as the representative value of the thickness of each specimen. Care was taken to apply as small pressures as possible to the specimen during measurement.

The tensile test was performed in the longitudinal direction of the specimen to investigate the mechanical properties of ITB. Sandpapers were glued to the top and bottom ends of the specimen to avoid slipping from clamps when the tissue was loaded (Henderson et al., 2015; Otsuka et al., 2018). A loading-unloading test was performed with a displacement-force measurement unit (ZTA-500N; EMX-1000N, Imada, Japan). Both top and bottom of the specimen were fixed to the clamps with 5 mm, respectively. The loading-unloading cycle was repeated 5 cycles at a speed of 25 mm/min (Henderson et al., 2015). The loading distance was set at 1.2-1.5 mm to calculate the linear region of the loading path. In each trial, the displacement (mm) and load (N) of the tissue were recorded using a software (Force Recorder Professional, Imada, Japan) in a personal computer at a sampling frequency of 1000 Hz. The specimens were kept moist throughout the tensile test by pipetting them with 50% alcohol (Otsuka et al., 2018; Shan et al., 2019).

Mechanical properties analysis

Since forces obtained from the first and second loading–unloading cycles (preconditioning) were substantially lower from other cycles (Shan et al., 2019), the third to fifth cycles were analyzed. The displacement-load relationship of the loading path in each cycle was divided into the toe region (change in load with respect to displacement was nonlinear), and the linear region (elongation and load changes were proportional). Linear region was identified based on the previous studies (Mogi et al., 2018; Shan et al., 2019). Loads were normalized to the maximum load and the displacements at every 5% of the relative loads were obtained. The transition from the toe to linear region was determined when the elongation of the tissue at every 5% of relative loads was constant at and above that point. The slope of the regression line from the displacement-load relationship in the linear region was defined as the stiffness (N/mm) of the tissue. In addition, stress (N/mm^2) and strain (%) was calculated from the following equations in line with our previous studies (Otsuka et al., 2018; Shan et al., 2019) (Fig.4-4).

Stress (N/mm^2) = F / A (1)

Strain (%) = ε / L (2)

Where F is the tensile load, A is the cross-sectional area of each specimen ε and L are the elongation of the ITB and its initial grip-to-grip length, respectively. Young's modulus (MPa) was also calculated from the slope of the same linear region of strain-stress relationship curve to measure the material property of ITB.

The mechanical hysteresis (%) was calculated from relationship between strain and stress to measure the viscoelastic property of ITB (Maganaris and Paul, 2000). The energy required to stretch the tissue (WS) and the energy released by the shortening of the tissue (WR) were calculated by integrating numerically the function of displacement upon loading and

unloading, respectively. The mechanical hysteresis in the loading-unloading cycle was calculated using the equation.

Hysteresis (%) = 100*(WS - WR) / WS (3)

4.2.3. Statistical analysis

Results are shown as mean and SDs. All statistical analyses were performed using a statistical software (IBM SPSS Statistics 23, IBM, Armonk, USA). Reliability was quantified by one-way random (average measure) intraclass correlation coefficients (ICC) of two repeated measurements of the SWV of ITB at each site and position. For *in vivo* test, a two-way ANOVA was conducted to analyze the effects of sites and positions on the SWV of ITB. The ANOVA was followed by post-hoc tests with Bonferroni correction. A one-way ANOVA was also performed to compare the morphological and mechanical properties of ITB among sites on cadavers, followed by a Bonferroni-corrected post-hoc test. The significance level was set at $p < 0.05$.

4.3. Results

4.3.1. *In vivo* study

Shear wave velocity of ITB

The ICC of SWV was 0.86 to 0.99 for each site and joint angle (Table 4-1), i.e., SWV of ITB was kept almost perfectly repeatable (Landis and Koch, 1977) in the two measurement cycles. There was a significant interaction between sites and positions ($p < 0.01$) (Fig.4-5). Higher values of ITB SWV was observed at the superior border of the patella (site 4; 3.3-9.3 m/s). On the other hand, ITB SWV values were lower over the distal site of VL (site 3; 2.4-8.0 m/s). ITB was stiffer at hip 0˚ /knee 90˚ (7.6-9.5 m/s) and more compliant at hip 90˚ /knee 0˚ (2.5-4.5 m/s).

4.3.2. Cadaveric study

Thickness

There was a tendency for ITB thickness becoming larger from the proximal toward the distal sites with significant differences in the middle part (0.81-2.45 mm on average) (Fig.4-6a).

No significant differences were noted within the proximal (sites 1-2) or distal (4-5) areas.

Mechanical properties of ITB

The stiffness of ITB between the distal end of femur and the proximal end of tibia (site 5; 118.8 ± 41.6 N/mm) was lower than other sites (over the proximal, middle, and distal sites of VL; 154.6-179.2 N/mm) ($p < 0.05$). At the superior border of the patella (site 4), ITB was more compliant than that over the distal end of VL (site 3) ($p = 0.01$) (Fig.4-6b). A tendency opposite to that of thickness was seen for the Young's modulus of ITB, higher to lower, proximal to distal. (site 1; 337.9 ± 103.3 MPa, site 2; 362.7 ± 50.5 MPa, as compared to other sites (68.8-73.7 MPa) ($p < 0.01$) (Fig.4-6c). On the other hand, the hysteresis of ITB mechanical property was most prominent in the middle (site 3; 29.1 ± 7.2% than other sites, 19.3-22.9%) ($p < 0.01$) (Fig.4-6d).

4.4. Discussion

Our *in vivo* study demonstrated sufficiently high ICC values of the SWV of ITB regardless of the sites or positions (ICC = 0.86-0.99), indicating reliability of the SWE measurements throughout the test. ITB was stiffer at the distal sites (site 4 and 5) and most compliant over the distal aspect of VL (site 3), which is partly in line with a recent cadaveric study (Wilhelm et al., 2017) but not with our *ex situ* cadaver observation. ITB inserts onto the bones at the knee joint where it can be exposed to considerable mechanical shear stress (Benjamin et al., 2006). Such mechanical stress accumulation might be related with the larger thickness and higher stiffness of ITB around the distal part (sites 4-5). Proximally, ITB originates from TFL and GM which contribute to various hip joint movements. The proximal sites (site 1 and 2) of ITB might be stretched by the attaching muscles crossing the hip, thereby showing higher stiffness than the distal aspect over VL (site 3) both in our *in vivo* and *ex situ* observations. In cadavers, the hysteresis of ITB at the site 3 was higher than other sites. This may also explain the lower stiffness

of ITB over the distal site of VL where the mechanical stress is dispersed, and the tissue is weakened in its material property. Interestingly, higher Young's moduli of ITB were noted proximally over VL (site 1-3) than the distal sites (site 4 and 5) in the cadaver measurement. Fairclough et al. (2007) reported that the distal part of ITB is "tendinous or ligamentous", while over VL it can be regarded as "deep fascia" (Otsuka et al., 2018). The existence of the fat pad and anterolateral capsule of the knee joint that has lower stiffness than ITB (Rahnemai-Azar et al., 2016) may explain the clear differences of the material property between fascial and tendinous and/or ligamentous parts of ITB. Difficulty in clear separation of these tissues in our cadaver measurement may be the reason for the difference from the *in vivo* observation.

Association of the combinations of the joint position combinations of the hip and knee with the ITB stiffness *in vivo*, was another significant finding of our study. As initially hypothesized, the configurations of the knee and hip joint angles did affect the mechanical properties of ITB. At most of the sites, ITB stiffness increased with hip extension and knee flexion, which follows previous reports demonstrating higher stiffness of ITB at the hip extended position using the same technique (Tateuchi et al., 2015, 2016). Previous studies reported that VL and TFL became stiffer by the passive knee flexion (Xu et al., 2018; Umehara et al., 2015). ITB receives anatomical connection of the fascicles of these muscles, thus might also be stretched passively according to their elongation by knee flexion. Furthermore, the distal aspects of ITB (site 4 and 5) was stiffer compared with other sites especially at the position of knee flexed at 25˚. A previous study found that the tension in the ITB causes its overall orientation to shift from anterior to posterior direction by knee flexion while moving onto the lateral epicondyle of the femur, thereby increasing its stiffness, which occurs when the knee is at 20-30˚ (Fairclough et al., 2006).

Furthermore, the present study clarified changes in ITB stiffness according to the alteration of hip along with the knee angles, which to the best of our knowledge is the first achievement over the existing studies. We revealed that the hip angle alteration remarkably affected the ITB stiffness more than that of the knee, regardless of sites. In other words, ITB can be stretched more easily by hip extension than knee flexion. This has important clinical relevance as described later in detail.

The ITB syndrome is an overuse injury which induces lateral and distal knee pain during exercise such as running and cycling (Holmes et al., 1993; Merlo and Migliorini, 2016). Previous studies showed that the ITB syndrome frequently occurs near the patella with the knee flexed by 20-30°, possibly due to the compressive stress between ITB and lateral femoral epicondyle (Orchard et al., 1996). Higher stiffness of the distal ITB at knee 25° shown in our *in vivo* study follows that finding. The differences of the stiffness between the distal site of VL (site 3; more compliant) and the tendinous part of ITB (site 4; stiffer) might be related to the frequent development of the ITB syndrome near the patella (Ibrahim et al., 2011). Although ITB at the superior aspect of the patella was stiffer with the knee positioned at 25° compared to 0°, there was no significant difference between knee 25° and further flexion. This suggests that the tensile stress on ITB is a function of not only the knee flexion but also the compressive stress. Furthermore, a recent study argued that the ITB syndrome occurs not only at the distal site but also around the proximal periphery of ITB (Decker and Hunt, 2018). Fairclough et al. (2007) suggested that the impaired function of hip musculature could be the reason for the ITB syndrome at the proximal region. The results of the present study support these studies and suggest that the hip joint angle changes are the important factor of the ITB stiffness, even in the passive condition.

Fredericson et al. (2000) concluded that the fascial adhesions of the posterior ITB to the lateral epicondyle of the femur can cause the distal ITB pain. Several works that followed showed that stretching ITB by hip/knee movements combined with the mechanical stimulation with massage are the useful treatments for the ITB syndrome (Fredericson et al., 2002, 2006). However, Brosseau et al. (2002) showed that the "fascial manipulation" (e.g. deep transverse friction massage superficially) showed no consistent benefit for the patients with ITB syndrome. The present study points to the notion that the site- and joint angle-specific approach with appropriate manual therapeutic treatment can lead to the treatment, and even prevention, of ITB syndrome.

There are several limitations of the present study. First of all, the specimens used for the tensile test was taken from formalin-fixed cadavers. Several previous studies used un-embalmed or fresh-frozen cadavers (Wilhelm et al., 2017; Rahnemai-Azar et al., 2016) to measure the mechanical properties of ligaments including ITB, and some findings showed alteration of the mechanical property of the ligaments due to embalming and freezing (Viidik and Lewin, 1966; Woo et al, 1986). The exact number of values of the present mechanical test may be different if we used other fixation methods. However, the fixation methods themselves should not systematically matter the site-differences of the ITB mechanical properties. In addition, in our *in vivo* study, the participants kept relaxed with no contraction of the muscles during measurement of the stiffness and we did not test active conditions. A recent study revealed that not only the muscles but also their surrounding structures (e.g. deep fascia) becomes stiffer with muscle contraction (Otsuka et al., 2019). Future studies will confirm the alterations of the ITB stiffness during exercise with joint angle changes, and may lead to further understanding of the mechanism of ITB related injuries.

4.5. Conclusion

Our study revealed that the mechanical properties of ITB was different between sites. We also demonstrated that both hip and knee joint angles affected stiffness of ITB, with the hip

angles remarkably affecting the values compared with the knee. These site- and joint angle-dependent mechanical properties of ITB could be related to the site-dependence of ITB injuries.
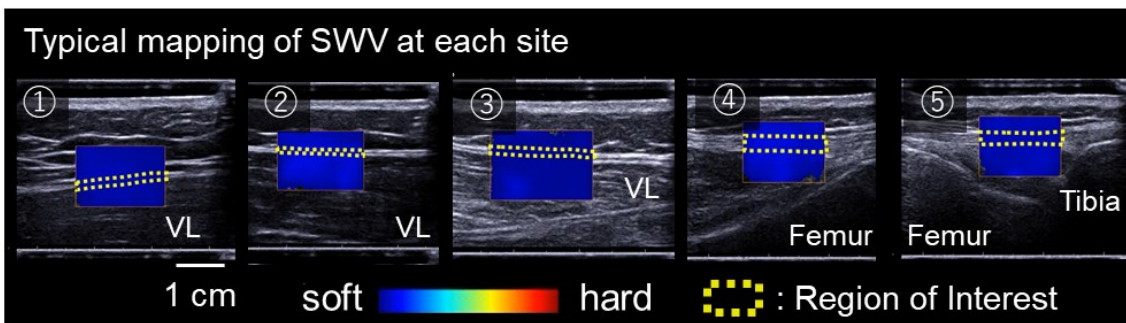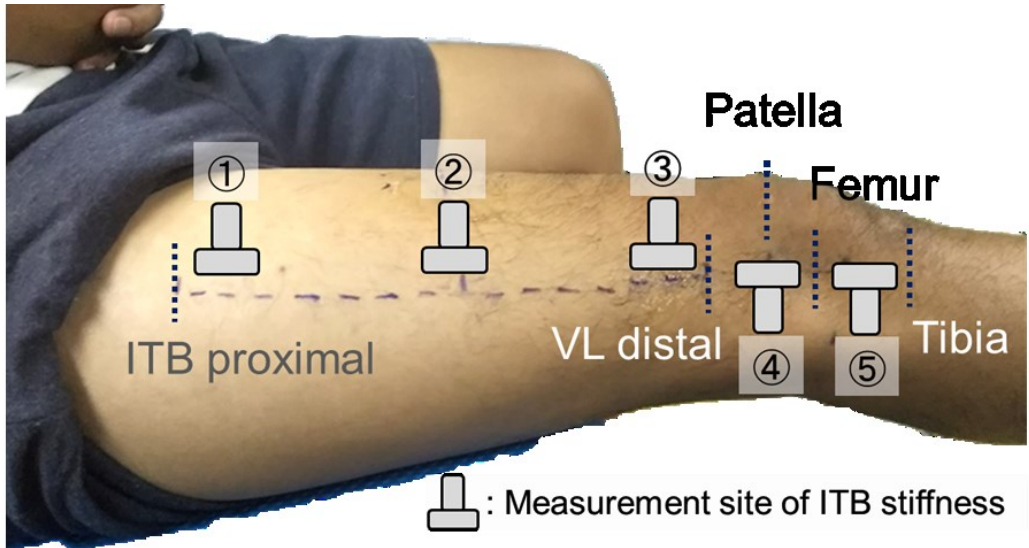
Fig. 4-1.

The photos showing measurement sites of the ultrasound shear wave elastography (SWE) and the typical mappings of the shear wave velocity (SWV). The transducer of SWE was placed on the skin over the proximal, medial, and distal sites of VL (site 1-3), superior boarder of patella (site 4), and midway of femur and tibia (site 5).
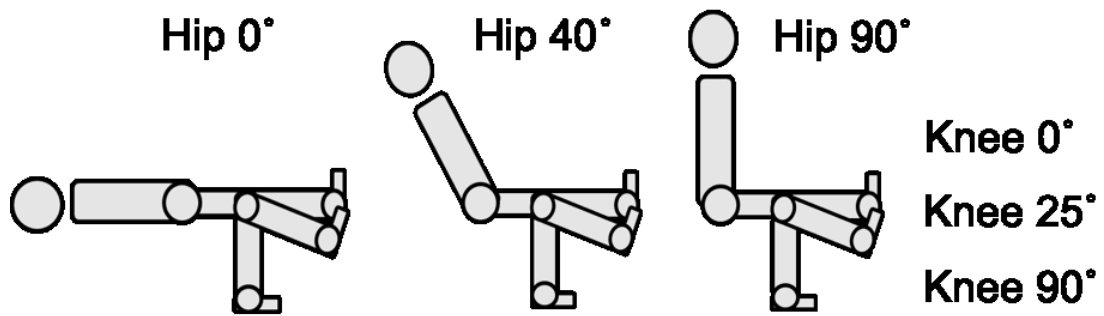
Fig. 4-2.

Measurements were conducted at nine different joint angle configurations which were the combination of knee (0˚, 25˚, 90˚) and hip (0˚, 40˚, 90˚) joint angles (0˚ being full extension of hip and knee), and ankle joint was kept at neutral position through the measurements.
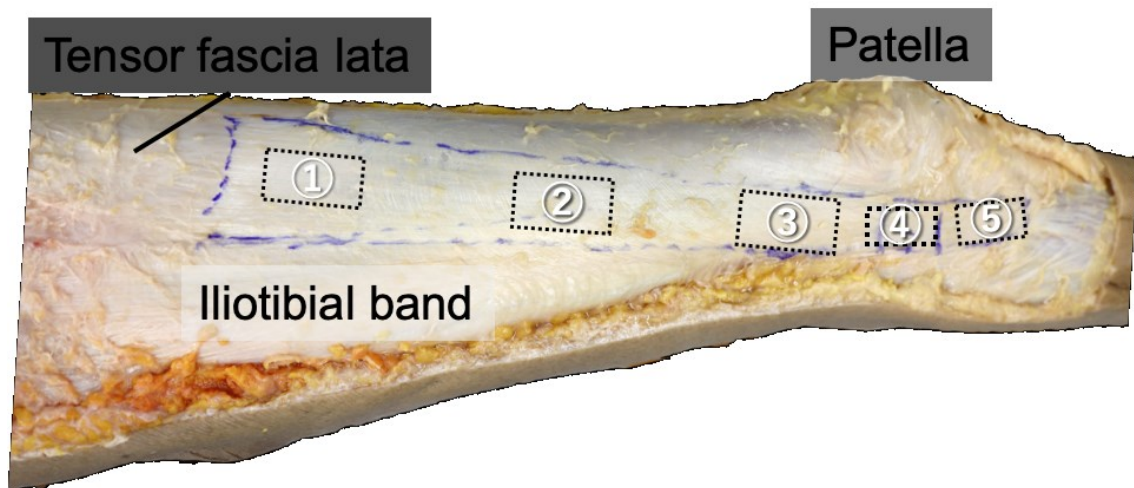
Fig. 4-3.

Specimens were taken from 5 different sites (over the proximal, medial, and distal sites of VL; site 1-3, superior boarder of patella; site 4, and midway of femur and tibia; site 5) of the cadaver's right leg. Specimens from site 1-3 were 2 x 4mm and site 4, 5 were 1 x 3mm in the transverse and longitudinal directions, respectively.
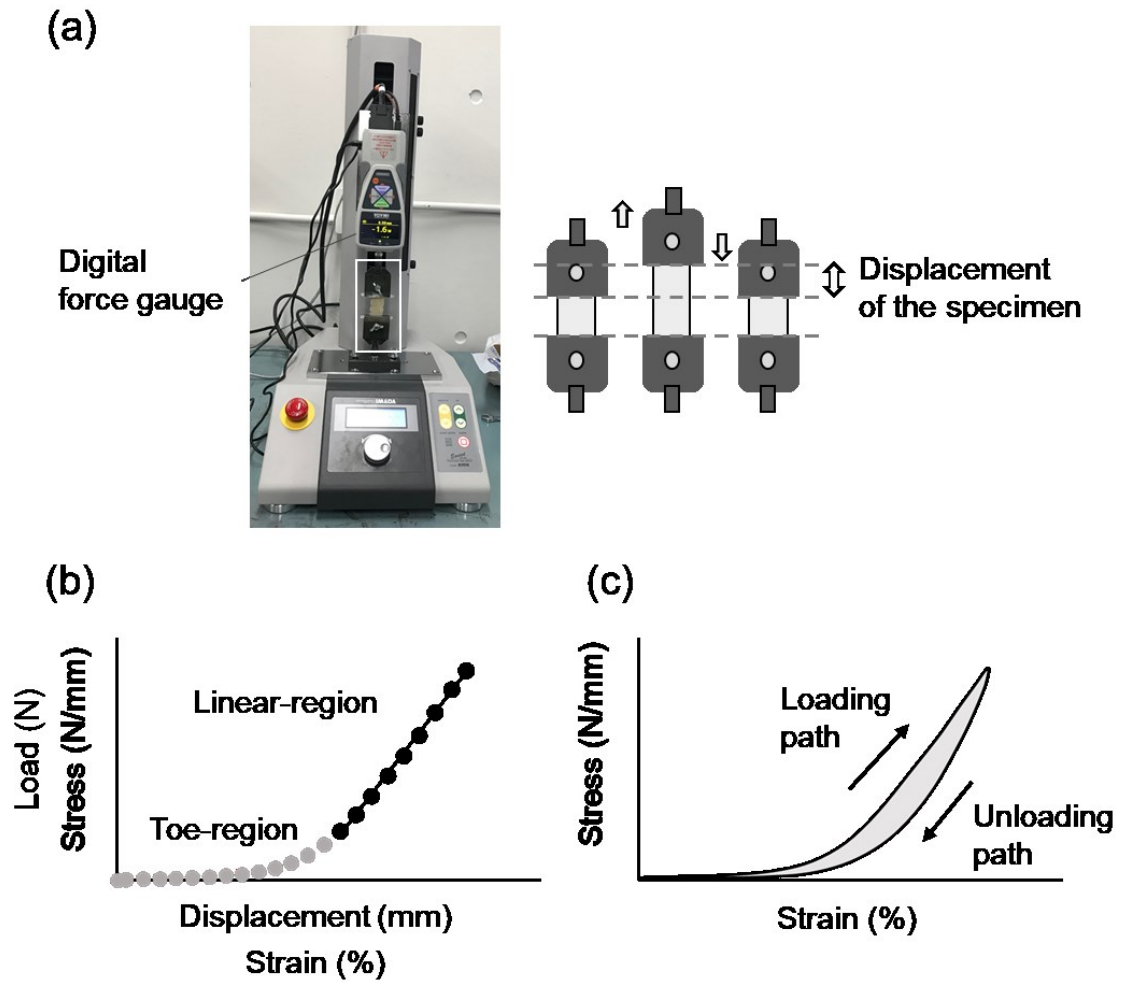
Fig. 4-4.

Tensile test was performed for each ITB specimen (a). Stiffness (b), Young's modulus (b), and hysteresis (c) were calculated from repeated loading-unloading cycles.

Table 4-1.

Repeatability of SWV of ITB from two cycles of measurements.

	Joint angle								
	Hip 0°			Hip 25°			Hip 90°		
	Knee 0°	Knee 25°	Knee 90°	Knee 0°	Knee 25°	Knee 90°	Knee 0°	Knee 25°	Knee 90°
site 1	0.995	0.978	0.992	0.972	0.975	0.992	0.863	0.958	0.990
site 2	0.993	0.993	0.995	0.922	0.998	0.992	0.984	0.992	0.979
site 3	0.993	0.998	0.970	0.920	0.997	0.996	0.981	0.969	0.988
site 4	0.992	0.980	0.982	0.984	0.980	0.962	0.990	0.996	0.994
site 5	0.997	0.987	0.981	0.999	0.988	0.990	0.994	0.994	0.994

Values show interclass correlation coefficients (ICC) values of shear wave velocity (SWV) of ITB at each site with each position.
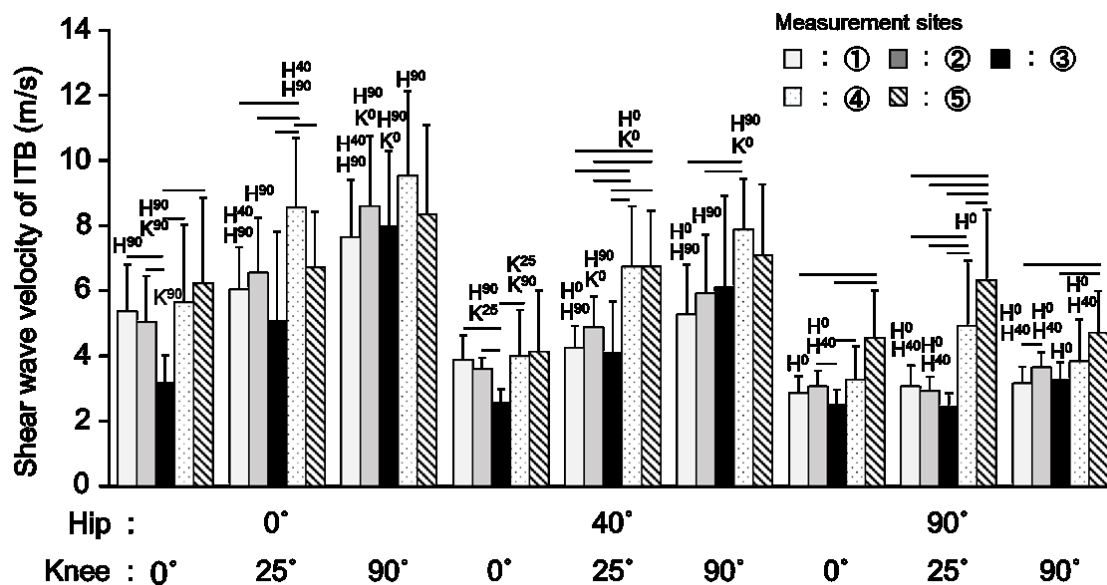
Fig. 4-5.

The SWV of ITB at each site and each position obtained from *in vivo* measurement. Values are presented mean ± SD. -: Significant differences between sites at $p < 0.05$. H^0, H^{40}, and H^{90} indicate significant differences compared with hip joint angle at 0, 40, and 90˚, respectively ($p < 0.05$). K^0, K^{25}, K^{90} indicate significant differences compared with knee joint angle at 0, 25, and 90˚ at $p < 0.05$.
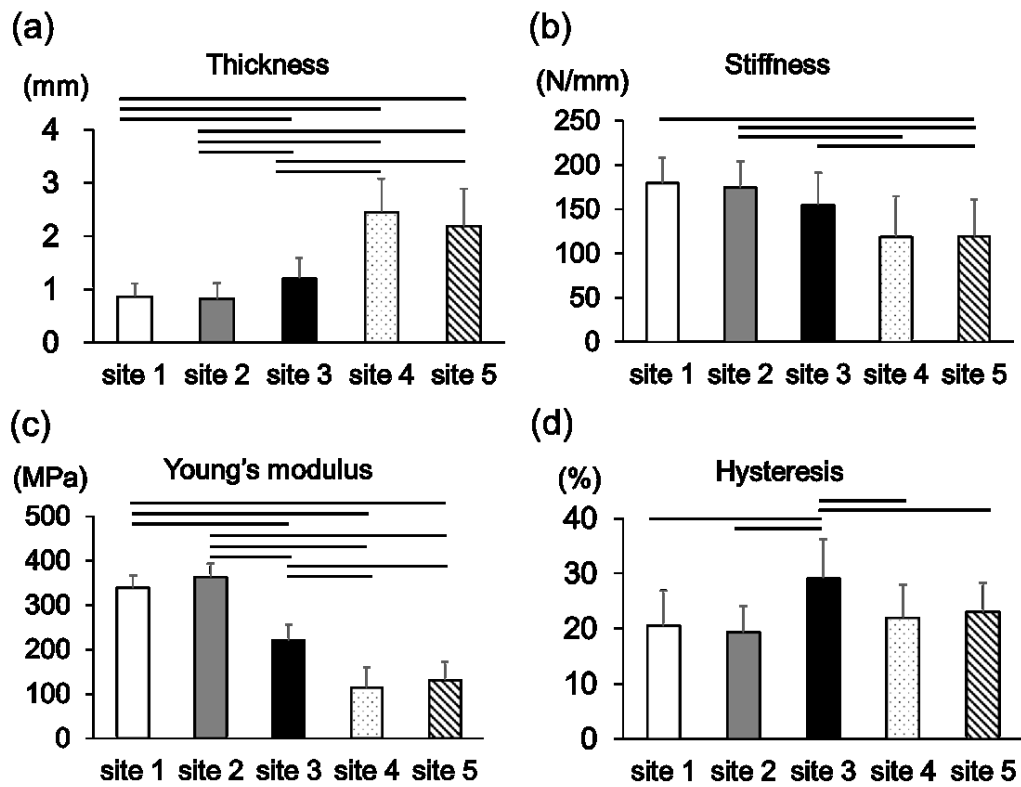
Fig. 4-6.

The thickness (a), stiffness (b), Young's modulus (c), and hysteresis (d) of ITB at each site from the tensile test of cadaveric specimens. Values are presented mean $\pm$ SD. -: Significant differences between sites at $p < 0.05$

CHAPTER 5

General discussion

5.1. Main findings of each chapter

In the present thesis, cadaveric studies were conducted to measure the morphological and mechanical properties of the deep fascia (including ITB) in detail. *In vivo* studies were also performed to investigate the behavior of the fascial structures during body movement (e.g. contraction and joint angle change). The main findings of each chapter in this thesis are as follows.

5.1.1. Chapter 2

1. The fascia lata showed site-dependent morphological properties. The fascia lata at the lateral site was thicker and rich in the longitudinal directed collagen fibers compared with that of other sites.

2. Site-dependent mechanical properties were also observed. The stiffness, Young's modulus, and hysteresis were higher at the lateral site of the fascia lata when it was stretched in the longitudinal direction.

3. Anisotropic mechanical properties of the fascia lata were demonstrated. The stiffness and Young's modulus of the fascia lata were much higher in the longitudinal direction than the transverse direction at every site.

4. At the medial site of the fascia lata, the distribution of the longitudinally directed fibers was higher in males than females, on the other hand, the distribution of transversely directed fibers was higher in females than males. No significant difference was observed in the thickness between males and females.

5.1.2. Chapter 3

1. No significant differences of the SWV were observed between RF and VL muscles. The SWV of the fascia lata over the VL was higher than that over the RF.

2. The quadriceps muscles and fascia lata became stiffer as increasing the level of knee extension torque exertion. In addition, the degree of stiffening of the quadriceps muscles and

fascia lata was higher in the longitudinal than the transverse direction.

3. The degree of stiffening of the muscles was higher compared with that of the fascia lata which means the muscles are more likely to become stiffer during contraction than the fascia lata.

5.1.3. Chapter 4

1. *Ex situ* study showed site-dependent morphological and mechanical properties of ITB. ITB showed higher ITB thickness at the distal sites than the middle and proximal sites. The ITB stiffness and Young's modulus were higher over the VL and lower at the distal sites. The hysteresis was higher at ITB over the distal site of VL than other sites.

2. *In vivo* study demonstrated that the SWV of ITB was higher at the superior border of the patella and lower over the distal site of VL.

3. The joint angle-dependent mechanical properties were also observed at *in vivo* study. ITB became stiffer associated with the hip extension and knee flexion. The highest SWV was observed at hip 0˚ and knee 90˚.

5.2. Generalization of the findings: Site- and direction-dependence of the fascial structures

By the cadaveric exmeriments in chapter 2, remarkable characteristics of the lateral site of the fascia lata were revealed (thicker, higher distribution of the longitudinally directed fibers, and stiffer than other sites). In addition to the site-dependence, the fascia lata showed anisotropic characteristics of the mechanical properties (stiffer in the longitudinal direction than the transverse direction). It can be considered that the differences of the distribution of the fiber directions and thickness between and within sites may induce the site-dependent and anisotropic mechanical properties of the fascia lata.

The site- and direction-dependent mechanical properties were also found in the *in vivo* study in chapter 3. The fascia lata over VL was stiffer than that over RF at rest and during contractions, which follows the finding in chapter 2, and further proves the alteration of deep fascia stiffness during motor performance. The fascia lata became stiffer associated with the increasing of contraction intensity, and the degree of stiffening was higher in the longitudinal than

the transverse direction. Interestingly, the degree of stiffening of the fascia lata was not different between RF and VL. These results suggest that the degree of stiffening of the fascia lata may be a function predominantly of contraction intensity of the underlying muscles, regardless of the morphological differences (e.g. thickness and fiber orientations) in the fascia lata.

From the *ex situ* and *in vivo* studies of chapter 2 and chapter 3, outstanding features of the lateral site of the fascia lata were observed. Therefore, in chapter 4, the morphological and mechanical properties of the thicker and stiffer part of the fascia lata (called ITB) were examined in detail. ITB showed higher thickness, but lower stiffness and Young's modulus at the distal site of cadaveric thigh, and was stiffer at the distal thigh of living human. The joint angle-dependence of the mechanical properties as well as the site-differences of ITB were observed. ITB became stiffer associated with hip extension and knee flexion.

The results of the present thesis imply that the morphological and mechanical properties of the fascial tissue are different between sites (even in the same segment of the body) according to mirror the characteristics of the underlying muscles (Marshall et al., 2011; Stecco and Stecco, 2012). Furthermore, the properties of the fascial tissue (e.g. stiffness) change by the muscle contractions and joint angle configurations, showing high plasticity of the fascial tissues.

5.3. Applicability of the finding: Interactions between muscles and deep fascia

Throughout the thesis, site-, direction-, and contraction intensity-dependent morphological and mechanical properties of the fascial tissues were examined. In particular, the lateral site of the fascia lata was rich in the longitudinally directed collagen fibers. Since the lateral site of the fascia lata connects to the TFL, GM, and VL muscles, the greater mechanical load should be imposed especially on the lateral site of the fascia lata during body movements. The force being exerted by the muscle contraction transmits to the deep fascia and the collagen fibers run along the direction of underlying and attaching muscles' contraction (Stecco et al., 2009; Stecco & Stecco, 2012). The greater mechanical stress by these large and strong muscles connected with the lateral site of the fascia lata may affect the higher distribution of the longitudinal directed collagen fibers of fascia lata at that region. Additionally, the mechanical properties of the fascia lata may reflect its morphological properties, thus the fascia lata was stiffer

when it pulled in the longitudinal direction than the transverse direction in the cadaveric study.

In vivo study in chapter 3 also showed clear direction-dependence of the mechanical property of the fascia lata (the degree of stiffening was higher in the longitudinal than the transverse of the probe direction). Although the fascia lata was stiffer than the muscles, the degree of stiffening of the fascia lata was lower compared with that of the underlying muscles in the longitudinal direction. As noted in the literature review, muscle fibers insert into the deep fascia and/or connected to it via epimysium. Through such connections, much amount of the force generated by the muscle contraction can be transmitted to the neighboring deep fascia (Rijkelijkhuizen et al., 2005). Therefore, it can be considered that the fascia lata becomes stiffer due to the passive mechanical stress induced by the contraction of underlying muscles through the myofascial network. In addition, the forces transmit not only in the direction of the muscle contraction but also the perpendicular direction of it (Maas and Sanderock, 2010; Findley et al., 2015). Because of these radial forces, deep fascia may become stiffer in the transverse direction. According to the stiff property in the longitudinal direction, the deep fascia can act as a spring which plays important roles in contributing elastic energy storage, myofascial transmission and limb stability as the tendon and aponeurosis (Kawakami et al., 2002; Shan et al., 2019). On the other hand, less stiffness of the deep fascia in the transverse direction could contribute to maintain intermuscular pressure and allow the underlying muscles to change their shape (e.g. bulging) during contraction (Iwanuma et al., 2011).

Due to the thick and stiff characteristics, the lateral site of the fascia lata is specially named ITB. ITB has the direct connections with the muscles and bones as the origins and insertions, thereby, it can be said that the ITB is independent with the fascia lata. Human ITB is developed than other anthropoids, suggesting adaptation to bipedal locomotion (Eng et al., 2015a; Pontzer, 2007). Several studies reported the unique functions of ITB, such as elastic energy storage (Eng et al., 2015b), dynamic joint stability (Schipplein and Andriacchi, 1991), and postural stability (Evans, 1979). ITB showed higher stiffness at hip extended position (chapter 4). The hip angle in human is more extended than other anthropoids during bi-pedal walking (Yamazaki and Ishida, 1984; Hogervorst and Vereecke, 2014). In human, higher stiffness of ITB of the stance leg at hip extended position may contribute to prevent the pelvic drop of the swing

leg during bipedal walking.

5.4. Conclusion of the thesis

In this thesis, site- and direction-dependence of the morphological and mechanical properties of the fascia lata and ITB were shown by the cadaveric study. Besides, the contraction intensity- and joint angle-dependent stiffness of the deep fascia and ITB were proven by the *in vivo* measurements. These characteristics of the fascial tissues may contribute to match and optimize underlying muscles' contraction as the muscle-fascia entity. At the same time, the site-dependent mechanical properties of ITB could be the reason of inducing region-specific injury by the repetitive movement. The results of the present thesis suggest that the fascial tissue works as one of the essential organs to determine human motor performance and physical conditioning.

5.5. Future directions

In the present thesis, characteristics of the deep fascia was measured from old cadavers and young males. The morphological and mechanical features of the deep fascia as well as the muscles and tendons have some possibility to degenerate site- and region-specifically by aging and training (Mogi et al., 2018; Maeo et al., 2018). To prove the plasticity of the fascial tissues, the morphological and mechanical properties of the facial tissues should be measured subjected to the people at various ages and exercise habits. The influence of the training should be also investigated. In addition, due to the inhomogeneous and anisotropy of the stiffness, the deep fascia may assist the underlying muscles' contraction. It is necessary to apply the knowledges of the characteristics of the deep fascia which were examined in this thesis and are going to be studied to the methodologies of improving human motor performance (e.g. manipulations, trainings, and garments).

From the view point of material mechanics, the mechanical properties of the soft tissue are influenced by the tensile speed and temperature (Ozkaya et al., 1998). For example, the soft tissue becomes stiffer when it loaded faster at lower temperature. However, almost all of the research including the present study examined the elastic and viscoelastic properties of the soft tissues (e.g. deep fascia and tendon) under the single condition (tensile test were conducted by

the single speed at the room temperature). To examine the mechanical properties of the deep fascia at the different conditions by *ex situ* (e.g. under different tensile sppeds and room temperatures) and *in vivo* (e.g. different speeds of joint angle movement at the isokinetic condition) studies may support us to explain how to behave the deep fascia at the various situations of human body movement. The estimation of the material property (e.g. coffisient of viscoelasticity) of the deep fascia at different sites based on the principle of the material mechanics would also help us to understand the mechanism of the differences of the amount of energy release of the deep fascia depending on sites.

Due to the connections between deep fascia and muscles, the alterations of the fascial tissue's property are induced followed by impaired mobility and pain (Stecco et al., 2013; Fairclough et al., 2007). Several treatment methods which approaching to the fascial tissue were used in the clinical field (e.g. Fascial tissue therapy, connective tissue manipulation, myofascial release and fascial manipulation) (Lambert et al., 2017). While these techniques contribute to reducing chronic pain and improving range of motion (Harper et al., 2019; Ichikawa et al., 2015; Ikeda et al., 2019), almost all of these methods are only based on the experiences of the clinicians. To control the intensity and direction of the manipulation depending on the sites according to the knowledge in this thesis, further improvement of the joint mobility and reduction of the myofascial pain could be expected.

References

1. Alkner, B.A., Tesch, P.A., Berg, H.E., 2000. Quadriceps EMG/force relationship in knee extension and leg press. Med Sci Sports Exerc 32, 459-463.

2. Andonian, P., Viallon, M., Le Goff, C., de Bourguignon, C., Tourel, C., Morel, J., Giardini, G., Gergele, L., Millet, G.P., Croisille, P., 2016. Shear-wave elastography assessments of quadriceps stiffness changes prior to, during and after prolonged exercise: A longitudinal study during an extreme mountain ultra-marathon. Plos One 11, 1-21.

3. Arda, K., Ciledag, N., Aktas, E., Aribas, B.K., Kose, K., 2011. Quantitative assessment of normal soft-tissue elasticity using shear-wave ultrasound elastography. AJR Am J Roentgenol 197, 532-536.

4. Ateş, F., Hug, F., Bouillard, K., Jubeau, M., Frappart, T., Couade, M., Bercoff, J., Nordez, A., 2015. Muscle shear elastic modulus is linearly related to muscle torque over the entire range of isometric contraction intensity. J Electromyogr Kinesiol 25, 703-708.

5. Ates, F., Temelli, Y., Yucesoy, C.A., 2013. Human spastic Gracilis muscle isometric forces measured intraoperatively as a function of knee angle show no abnormal muscular mechanics. Clin Biomech 28, 48-54.

6. Ates, F., Temelli, Y., Yucesoy, C.A., 2014. Intraoperative experiments show relevance of inter-antagonistic mechanical interaction for spastic muscle's contribution to joint movement disorder. Clin Biomech 29, 943-949.

7. Ates, F., Temelli, Y., Yucesoy, C.A., 2016. The mechanics of activated semitendinosus are not representative of the pathological knee joint condition of children with cerebral palsy. J Electromyogr Kinesiol 28, 130-136.

8. Aubry, S., Risson, J.R., Kastler, A., Barbier-Brion, B., Siliman, G., Runge, M., Kastler, B., 2013. Biomechanical properties of the calcaneal tendon *in vivo* assessed by transient shear wave elastography. Skeletal Radiol 42, 1143-1150.

9. Azizi, E., Roberts, T.J., 2009. Biaxial strain and variable stiffness in aponeuroses. J Physiol

587, 4309-4318.

10. Benetazzo, L., Bizzego, A., De Caro, R., Frigo, G., Guidolin, D., Stecco, C., 2011. 3D reconstruction of the crural and thoracolumbar fasciae. Surg Radiol Anat 33, 855-862.

11. Benjamin, M., 2009. The fascia of the limbs and back-a review. J Anat 214, 1-18.

12. Benjamin, M., Toumi, H., Ralphs, J.R., Bydder, G., Best, T.M., Milz, S., 2006. Where tendons and ligaments meet bone: attachment sites ('entheses') in relation to exercise and/or mechanical load. J Anat 208, 471-490.

13. Bennett, M.B., Ker, R.F., Dimery, N.J., Alexander, R.M., 1986. Mechanical-Properties of Various Mammalian Tendons. J Zool 209, 537-548.

14. Birnbaum, K., Siebert, C.H., Pandorf, T., Schopphoff, E., Prescher, A., Niethard, F.U., 2004. Anatomical and biomechanical investigations of the iliotibial tract. Surg Radiol Anat 26, 433-446.

15. Blasi, M., Blasi, J., Domingo, T., Perez-Bellmunt, A., Miguel-Perez, M., 2015. Anatomical and histological study of human deep fasciae development. Surg Radiol Anat 37, 571-578.

16. Bogduk, N., Macintosh, J.E., 1984. The Anatomy of the Thoracolumbar Fascia. Journal of Anatomy 139, 195-195.

17. Brum, J., Bernal, M., Gennisson, J.L., Tanter, M., 2014. *In vivo* evaluation of the elastic anisotropy of the human Achilles tendon using shear wave dispersion analysis. Phys Med Biol 59, 505-523.

18. Carvalhais, V.O., Ocarino Jde, M., Araujo, V.L., Souza, T.R., Silva, P.L., Fonseca, S.T., 2013. Myofascial force transmission between the latissimus dorsi and gluteus maximus muscles: an *in vivo* experiment. J Biomech 46, 1003-1007.

19. Cruz-Montecinos, C., Cerda, M., Sanzana-Cuche, R., Martin-Martin, J., Cuesta-Vargas, A., 2016. Ultrasound assessment of fascial connectivity in the lower limb during maximal cervical flexion: technical aspects and practical application of automatic tracking. BMC Sports Sci Med Rehabil 8, 18.

20. Cutts, A., Seedhom, B.B., 1993. Validity of cadaveric data for muscle physiological cross-sectional area ratios: a comparative study of cadaveric and *in-vivo* data in human thigh muscles. Clin Biomech 8, 156-162.

21. Day, J.A., Copetti, L., Rucli, G., 2012. From clinical experience to a model for the human fascial system. J Bodyw Mov Ther 16, 372-380.

22. Day, J.A., Stecco, C., Stecco, A., 2009. Application of Fascial Manipulation technique in chronic shoulder pain-anatomical basis and clinical implications. J Bodyw Mov Ther 13, 128-135.

23. De Coninck, K., Hambly, K., Dickinson, J.W., Passfield, L., 2018. Measuring the morphological characteristics of thoracolumbar fascia in ultrasound images: an inter-rater reliability study. BMC Musculoskelet Disord 19, 180.

24. Decker, G., Hunt, D., 2018. Proximal iliotibial syndrome in a runner: a case report. Phys Med Rehabil 11, 206-209.

25. Ema, R., Wakahara, T., Yanaka, T., Kanehisa, H., Kawakami, Y., 2016. Unique muscularity in cyclists' thigh and trunk: A cross-sectional and longitudinal study. Scand J Med Sci Sports 26, 782-793.

26. Eng, C.M., Arnold, A.S., Biewener, A.A., Lieberman, D.E., 2015a. The human iliotibial band is specialized for elastic energy storage compared with the chimp fascia lata. J Exp Biol 218, 2382-2393.

27. Eng, C.M., Arnold, A.S., Lieberman, D.E., Biewener, A.A., 2015b. The capacity of the human iliotibial band to store elastic energy during running. J Biomech 48, 3341-3348.

28. Eng, C.M., Roberts, T.J., 2018. Aponeurosis influences the relationship between muscle gearing and force. J Appl Physiol 125, 513-519.

29. Enomae, T., 2005. Novel technique for analyzing physical properties of paper using image processing. Japan J Paper Technol 48, 1-5.

30. Evans, P., 1979. The postural function of the iliotibial tract. Ann R Coll Surg Engl 61, 271-

280.

31. Fairclough, J., Hayashi, K., Toumi, H., Lyons, K., Bydder, G., Phillips, N., Best, T.M., Benjamin, M., 2006. The functional anatomy of the iliotibial band during flexion and extension of the knee: implications for understanding iliotibial band syndrome. J Anat 208, 309-316.

32. Fairclough, J., Hayashi, K., Toumi, H., Lyons, K., Bydder, G., Phillips, N., Best, T.M., Benjamin, M., 2007. Is iliotibial band syndrome really a friction syndrome? J Sci Med Sport 10, 74-78.

33. Findley, T., Chaudhry, H., Dhar, S., 2015. Transmission of muscle force to fascia during exercise. J Bodyw Mov Ther 19, 119-123.

34. Fukunaga, T., Kawakami, Y., Kubo, K., Kanehisa, H., 2002. Muscle and tendon interaction during human movements. Exerc Sport Sci Rev 30, 106-110.

35. Garfin, S.R., Tipton, C.M., Mubarak, S.J., Woo, S.L., Hargens, A.R., Akeson, W.H., 1981. Role of fascia in maintenance of muscle tension and pressure. J Appl Physiol Respir Environ Exerc Physiol 51, 317-320.

36. Gaudreault, N., Boyer-Richard, É., Fede, C., Fan, C., Macchi, V., De Caro, R., Stecco, C., 2018. Static and dynamic ultrasound imaging of the iliotibial band/fascia lata: brief review of current literature and gaps in knowledge. Current Radiology Reports 6, 37.

37. Gulick, D.T., 2014. Influence of instrument assisted soft tissue treatment techniques on myofascial trigger points. J Bodyw Mov Ther 18, 602-607.

38. Gyaran, I.A., Spiezia, F., Hudson, Z., Maffulli, N., 2011. Sonographic measurement of iliotibial band thickness: an observational study in healthy adult volunteers. Knee Surg Sports Traumatol Arthrosc 19, 458-461.

39. Harper, B., Steinbeck, L., Aron, A., 2019. Fascial manipulation vs. standard physical therapy practice for low back pain diagnoses: A pragmatic study. J Bodyw Mov Ther 23, 115-121.

40. Henderson, E.R., Friend, E.J., Toscano, M.J., Parsons, K.J., Tarlton, J.F., 2015.

Biomechanical comparison of canine fascia lata and thoracolumbar fascia: an in vitro evaluation of replacement tissues for body wall reconstruction. Vet Surg 44, 126-134.

41. Hogervorst, T., Vereecke, E.E., 2014. Evolution of the human hip. Part 1: the osseous framework. Journal of hip preservation surgery 1, 39-45.

42. Holmes, J.C., Pruitt, A.L., Whalen, N.J., 1993. Iliotibial band syndrome in cyclists. Am J Sports Med 21, 419-424.

43. Horton, M.G., Hall, T.L., 1989. Quadriceps femoris muscle angle: normal values and relationships with gender and selected skeletal measures. Phys Ther 69, 897-901.

44. Huijing, P.A., 2007. Epimuscular myofascial force transmission between antagonistic and synergistic muscles can explain movement limitation in spastic paresis. J Electromyogr Kinesiol 17, 708-724.

45. Huijing, P.A., 2009. Epimuscular myofascial force transmission: a historical review and implications for new research. International Society of Biomechanics Muybridge Award Lecture, Taipei, 2007. J Biomech 42, 9-21.

46. Huijing, P.A., Baan, G.C., 2003. Myofascial force transmission: muscle relative position and length determine agonist and synergist muscle force. J Appl Physiol (1985) 94, 1092-1107.

47. Huijing, P.A., Van de Langenberg, R.W., Meesters, J.J., Baan, G.C., 2007. Extramuscular myofascial force transmission also occurs between synergistic muscles and antagonistic muscles. J Electromyogr Kinesiol 17, 680-689.

48. Huijing, P.A., Yaman, A., Ozturk, C., Yucesoy, C.A., 2011. Effects of knee joint angle on global and local strains within human triceps surae muscle: MRI analysis indicating *in vivo* myofascial force transmission between synergistic muscles. Surg Radiol Anat 33, 869-879.

49. Hwang, S.W., Nam, Y.S., Hwang, K., Han, S.H., 2012. Thickness and tension of the gluteal aponeurosis and the implications for subfascial gluteal augmentation. J Anat 221, 69-72.

50. Ichikawa, K., Takei, H., Mitomo, S., Ogawa, D., Hideyuki, 2015. Comparative analysis of ultrasound changes in the vastus lateralis muscle following myofascial release and

thermotherapy: A pilot study. Journal of Bodywork and Movement Therapies 19, 327-336.

51. Ikeda, N., Otsuka, S., Kawanishi, Y., Kawakami, Y., 2019. Effects of Instrument-assisted Soft Tissue Mobilization on Musculoskeletal Properties. Med Sci Sports Exerc 51, 2166-2172.

52. Iwanuma, S., Akagi, R., Kurihara, T., Ikegawa, S., Kanehisa, H., Fukunaga, T., Kawakami, Y., 2011. Longitudinal and transverse deformation of human Achilles tendon induced by isometric plantar flexion at different intensities. J Appl Physiol 110, 1615-1621.

53. Kanehisa, H., Ishiguro, N., Takeshita, K., Kawakami, Y., Kuno, S., Miyatani, M., Fukunaga, T., 2006. Effects of gender on age-related changes in muscle thickness in the elderly. International Journal of Sports and Health Science 4, 427-434.

54. Kaplan, E.B., 1958. The iliotibial tract: clinical and morphological significance. J Bone Joint Surg Am 40, 817-832.

55. Kawakami, Y., 2012. Morphological and functional characteristics of the muscle tendon unit. J Phys Fitness Sports Med 1, 287-296.

56. Kawakami, Y., Muraoka, T., Ito, S., Kanehisa, H., Fukunaga, T., 2002. *In vivo* muscle fibre behaviour during counter-movement exercise in humans reveals a significant role for tendon elasticity. J Physiol 540, 635-646.

57. Kern, D.S., Semmler, J.G., Enoka, R.M., 2001. Long-term activity in upper- and lower-limb muscles of humans. J Appl Physiol 91, 2224-2232.

58. Krause, F., Wilke, J., Vogt, L., Banzer, W., 2016. Intermuscular force transmission along myofascial chains: a systematic review. J Anat 228, 910-918.

59. Kubo, K., Kanehisa, H., Ito, M., Fukunaga, T., 2001a. Effects of isometric training on the elasticity of human tendon structures *in vivo*. J Appl Physiol 91, 26-32.

60. Kubo, K., Kanehisa, H., Kawakami, Y., Fukunaga, T., 2000. Elasticity of tendon structures of the lower limbs in sprinters. Acta Physiol Scand 168, 327-335.

61. Kubo, K., Kanehisa, H., Kawakami, Y., Fukunaga, T., 2001b. Influence of static stretching

on viscoelastic properties of human tendon structures *in vivo*. J Appl Physiol 90, 520-527.

62. Kubo, K., Ohgo, K., Takeishi, R., Yoshinaga, K., Tsunoda, N., Kanehisa, H., Fukunaga, T., 2006. Effects of isometric training at different knee angles on the muscle-tendon complex *in vivo*. Scand J Med Sci Sports 16, 159-167.

63. Kumar, P., Pandey, A.K., Kumar, B., Aithal, S.K., 2011. Anatomical study of superficial fascia and localized fat deposits of abdomen. Indian J Plast Surg 44, 478-483.

64. Kumka, M., Bonar, J., 2012. Fascia: a morphological description and classification system based on a literature review. J Can Chiropr Assoc 56, 179-191.

65. Lacourpaille, L., Hug, F., Bouillard, K., Hogrel, J.Y., Nordez, A., 2012. Supersonic shear imaging provides a reliable measurement of resting muscle shear elastic modulus. Physiol Meas 33, 19-28.

66. Lambert, M., Hitchcock, R., Lavallee, K., Hayford, E., Morazzini, R., Wallace, A., Conroy, D., Cleland, J., 2017. The effects of instrument-assisted soft tissue mobilization compared to other interventions on pain and function: a systematic review. Phys Ther Rev 22, 76-85.

67. Landis, J.R., Koch, G.G., 1977. The measurement of observer agreement for categorical data. Biometrics 33, 159-174.

68. Laudner, K., Compton, B.D., McLoda, T.A., Walters, C.M., 2014. Acute effects of instrument assisted soft tissue mobilization for improving posterior shoulder range of motion in collegiate baseball players. Int J Sports Phys Ther 9, 1-7.

69. Luomala, T., Pihlman, M., Heiskanen, J., Stecco, C., 2014. Case study: could ultrasound and elastography visualized densified areas inside the deep fascia? J Bodyw Mov Ther 18, 462-468.

70. Maas, H., Sandercock, T.G., 2010. Force transmission between synergistic skeletal muscles through connective tissue linkages. J Biomed Biotechnol 2010, 575672.

71. Maeo, S., Saito, A., Otsuka, S., Shan, X., Kanehisa, H., Kawakami, Y., 2018. Localization of muscle damage within the quadriceps femoris induced by different types of eccentric

exercises. Scand J Med Sci Sports 28, 95-106.

72. Maganaris, C.N., Paul, J.P., 2000. Hysteresis measurements in intact human tendon. J Biomech 33, 1723-1727.

73. Marinho, H.V.R., Amaral, G.M., Moreira, B.S., Santos, T.R.T., Magalhaes, F.A., Souza, T.R., Fonseca, S.T., 2017. Myofascial force transmission in the lower limb: An *in vivo* experiment. J Biomech 63, 55-60.

74. Markovic, G., 2015. Acute effects of instrument assisted soft tissue mobilization vs. foam rolling on knee and hip range of motion in soccer players. J Bodyw Mov Ther 19, 690-696.

75. Marshall, R., 2001. Living anatomy: Structure as the mirror of function, in: Press, M.U. (Ed.), Melbourne.

76. Maruyama, Y., Iizuka, S., Yoshida, K., 1991. Ultrasonic observation on distribution of subcutaneous fat in Japanese young adults with reference to sexual difference. Ann Physiol Anthropol 10, 61-70.

77. McCombe, D., Brown, T., Slavin, J., Morrison, W.A., 2001. The histochemical structure of the deep fascia and its structural response to surgery. J Hand Surg-Brit Eur 26, 89-97.

78. Mechelli, F., Arendt-Nielsen, L., Stokes, M., Agyapong-Badu, S., 2019. Validity of Ultrasound Imaging Versus Magnetic Resonance Imaging for Measuring Anterior Thigh Muscle, Subcutaneous Fat, and Fascia Thickness. Methods Protoc 2.

79. Merlo, M., Migliorini, S., 2016. Iliotibial band syndrome (ITBS), in: Bisciotti, G., Volpi, P., (Ed.), The lower limb tendinopathies, 3rd ed. Springer, Cham, Switzerland, pp. 117-126.

80. Mogi, Y., Torii, S., Kawakami, Y., Yanai, T., 2013. Morphological and mechanical properties of the Achilles tendon in adolescent boys. Japanese J phys Fitness Sports Med 62, 303-313.

81. Mogi, Y., Torii, S., Kawakami, Y., Yanai, T., 2018. A cross-sectional study on the mechanical properties of the Achilles tendon with growth. Eur J Appl Physiol 118, 185-194.

82. Noble, C.A., 1980. Iliotibial band friction syndrome in runners. Am J Sports Med 8, 232-

234.

83. Nordez, A., Hug, F., 2010. Muscle shear elastic modulus measured using supersonic shear imaging is highly related to muscle activity level. J Appl Physiol 108, 1389-1394.

84. Orchard, J.W., Fricker, P.A., Abud, A.T., Mason, B.R., 1996. Biomechanics of iliotibial band friction syndrome in runners. Am J Sports Med 24, 375-379.

85. Otsuka, S., Shan, X., Kawakami, Y., 2019. Dependence of muscle and deep fascia stiffness on the contraction levels of the quadriceps: An *in vivo* supersonic shear-imaging study. J Electromyogr Kinesiol 45, 33-40.

86. Otsuka, S., Yakura, T., Ohmichi, Y., Ohmichi, M., Naito, M., Nakano, T., Kawakami, Y., 2018. Site specificity of mechanical and structural properties of human fascia lata and their gender differences: A cadaveric study. J Biomech 77, 69-75.

87. Ozkaya, N., Nordin, M., Goldsheyder, D., Leger, D., 2012. Fundamentals of biomechanics. Springer.

88. Pontzer, H., 2007. Effective limb length and the scaling of locomotor cost in terrestrial animals. J Exp Biol 210, 1752-1761.

89. Proske, U., Morgan, D.L., 1987. Tendon Stiffness - Methods of Measurement and Significance for the Control of Movement - a Review. Journal of Biomechanics 20, 75-82.

90. Rahnemai-Azar, A.A., Miller, R.M., Guenther, D., Fu, F.H., Lesniak, B.P., Musahl, V., Debski, R.E., 2016. Structural properties of the anterolateral capsule and iliotibial band of the knee. Am J Sports Med 44, 892-897.

91. Rijkelijkhuizen, J.M., Baan, G.C., de Haan, A., de Ruiter, C.J., Huijing, P.A., 2005. Extramuscular myofascial force transmission for in situ rat medial gastrocnemius and plantaris muscles in progressive stages of dissection. J Exp Biol 208, 129-140.

92. Ryu, J., Jeong, W.K., 2017. Current status of musculoskeletal application of shear wave elastography. Ultrasonography 36, 185-197.

93. Sasaki, K., Toyama, S., Ishii, N., 2014. Length-force characteristics of *in vivo* human muscle reflected by supersonic shear imaging. J Appl Physiol 117, 153-162.

94. Sawai, S., Sanematsu, H., Kanehisa, H., Tsunoda, N., Fukunaga, T., 2006. Sexual-related difference in the level of muscular activity of trunk and lower limb during basic daily life actions. Jpn J Phys Fit Sport 55, 247-257.

95. Schipplein, O.D., Andriacchi, T.P., 1991. Interaction between active and passive knee stabilizers during level walking. J Orthop Res 9, 113-119.

96. Schleip, R., Jager, H., Klingler, W., 2012. What is 'fascia'? A review of different nomenclatures. J Bodyw Mov Ther 16, 496-502.

97. Shan, X., Otsuka, S., Yakura, T., Naito, M., Nakano, T., Kawakami, Y., 2019. Morphological and mechanical properties of the human triceps surae aponeuroses taken from elderly cadavers: Implications for muscle-tendon interactions. PLoS One 14, 1-18.

98. Shiina, T., Nightingale, K.R., Palmeri, M.L., Hall, T.J., Bamber, J.C., Barr, R.G., Castera, L., Choi, B.I., Chou, Y.H., Cosgrove, D., Dietrich, C.F., Ding, H., Amy, D., Farrokh, A., Ferraioli, G., Filice, C., Friedrich-Rust, M., Nakashima, K., Schafer, F., Sporea, I., Suzuki, S., Wilson, S., Kudo, M., 2015. Wfumb Guidelines and Recommendations for Clinical Use of Ultrasound Elastography: Part 1: Basic Principles and Terminology. Ultrasound in Medicine and Biology 41, 1126-1147.

99. Shiotani, H., Yamashita, R., Mizokuchi, T., Naito, M., Kawakami, Y., 2019. Site- and sex-differences in morphological and mechanical properties of the plantar fascia: A supersonic shear imaging study. Journal of Biomechanics 85, 198-203.

100. Sogabe, A., Mukai, N., Miyakawa, S., Mesaki, N., Maeda, K., Yamamoto, T., Gallagher, P.M., Schrager, M., Fry, A.C., 2009. Influence of knee alignment on quadriceps cross-sectional area. J Biomech 42, 2313-2317.

101. Stecco, A., Gilliar, W., Hill, R., Fullerton, B., Stecco, C., 2013. The anatomical and functional relation between gluteus maximus and fascia lata. J Bodyw Mov Ther 17, 512-517.

102. Stecco, A., Macchi, V., Masiero, S., Porzionato, A., Tiengo, C., Stecco, C., Delmas, V., De Caro, R., 2009a. Pectoral and femoral fasciae: common aspects and regional specializations. Surg Radiol Anat 31, 35-42.

103. Stecco, A., Masiero, S., Macchi, V., Stecco, C., Porzionato, A., De Caro, R., 2009b. The pectoral fascia: anatomical and histological study. J Bodyw Mov Ther 13, 255-261.

104. Stecco, C., Macchi, V., Porzionato, A., Duparc, F., De Caro, R., 2011. The fascia: the forgotten structure. Ital J Anat Embryol 116, 127-138.

105. Stecco, C., Pavan, P., Pachera, P., De Caro, R., Natali, A., 2014. Investigation of the mechanical properties of the human crural fascia and their possible clinical implications. Surg Radiol Anat 36, 25-32.

106. Stecco, C., Pavan, P.G., Porzionato, A., Macchi, V., Lancerotto, L., Carniel, E.L., Natali, A.N., De Caro, R., 2009c. Mechanics of crural fascia: from anatomy to constitutive modelling. Surg Radiol Anat 31, 523-529.

107. Stecco, C., Porzionato, A., Lancerotto, L., Stecco, A., Macchi, V., Day, J.A., De Caro, R., 2008. Histological study of the deep fasciae of the limbs. J Bodyw Mov Ther 12, 225-230.

108. Stecco, C., Stecco, A., 2012. Deep fascia of the lower limbs, in: Schleip, R., Findley, T.W., Chaitow, L., Huijing, P.A. (Eds.), Fascia: the tensional network of the human body. Elsevier, Edinburgh, p.33.

109. Stenroth, L., Peltonen, J., Cronin, N.J., Sipila, S., Finni, T., 2012. Age-related differences in Achilles tendon properties and triceps surae muscle architecture *in vivo*. J Appl Physiol 113, 1537-1544.

110. Tateuchi, H., Shiratori, S., Ichihashi, N., 2015. The effect of angle and moment of the hip and knee joint on iliotibial band hardness. Gait Posture 41, 522-528.

111. Tateuchi, H., Shiratori, S., Ichihashi, N., 2016. The effect of three-dimensional postural change on shear elastic modulus of the iliotibial band. J Electromyogr Kinesiol 28, 137-142.

112. Terry, G.C., Hughston, J.C., Norwood, L.A., 1986. The anatomy of the iliopatellar band and

iliotibial tract. Am J Sports Med 14, 39-45.

113. Umehara, J., Ikezoe, T., Nishishita, S., Nakamura, M., Umegaki, H., Kobayashi, T., Fujita, K., Ichihashi, N., 2015. Effect of hip and knee position on tensor fasciae latae elongation during stretching: An ultrasonic shear wave elastography study. Clin Biomech 30, 1056-1059.

114. Vieira, E.L., Vieira, E.A., da Silva, R.T., Berlfein, P.A., Abdalla, R.J., Cohen, M., 2007. An anatomic study of the iliotibial tract. Arthroscopy 23, 269-274.

115. Viidik, A., Lewin, T., 1966. Changes in tensile strength characteristics and histology of rabbit ligaments induced by different modes of postmortal storage. Acta Orthop Scand 37, 141-155.

116. Wilhelm, M., Matthijs, O., Browne, K., Seeber, G., Matthijs, A., Sizer, P.S., Brismee, J.M., James, C.R., Gilbert, K.K., 2017. Deformation response of the iliotibial band-tensor fascia lata complex to clinical-grade longitudinal tension loading in-vitro. Int J Sports Phys Ther 12, 16-24.

117. Wilke, J., Schleip, R., Yucesoy, C.A., Banzer, W., 2018. Not merely a protective packing organ? A review of fascia and its force transmission capacity. J Appl Physiol 124, 234-244.

118. Woo, S.L., Orlando, C.A., Camp, J.F., Akeson, W.H., 1986. Effects of postmortem storage by freezing on ligament tensile behavior. J Biomech 19, 399-404.

119. Wu, C.H., Chang, K.V., Mio, S., Chen, W.S., Wang, T.G., 2011. Sonoelastography of the Plantar Fascia. Radiology 259, 502-507.

120. Wu, C.H., Chen, W.S., Y., P.G., Wang, T.G., Lew, H.L., 2012. Musculoskeletral sonoelastography: A focused review of its diagnostic applications for evaluating tendons and fascia. J Medical Ultrasound 20, 79-86.

121. Xu, J.F., Hug, F., Fu, S.N., 2018. Stiffness of individual quadriceps muscle assessed using ultrasound shear wave elastography during passive stretching. J Sport Health Sci 7, 245-249.

122. Yahia, L.H., Pigeon, P., Desrosiers, E.A., 1993. Viscoelastic Properties of the Human Lumbodorsal Fascia. J Biomed Eng 15, 425-429.

123. Yamazaki, N., Ishida, H., 1984. A biomechanical study of vertical climbing and bipedal walking in gibbons. Journal of Human Evolution 13, 563-571.

124. Yoshitake, Y., Takai, Y., Kanehisa, H., Shinohara, M., 2014. Muscle shear modulus measured with ultrasound shear-wave elastography across a wide range of contraction intensity. Muscle Nerve 50, 103-113.

125. Yoshitake, Y., Uchida, D., Hirata, K., Mayfield, D.L., Kanehisa, H., 2018. Mechanical interaction between neighboring muscles in human upper limb: Evidence for epimuscular myofascial force transmission in humans. J Biomech 74, 150-155.

126. Yucesoy, C.A., 2010. Epimuscular myofascial force transmission implies novel principles for muscular mechanics. Exerc Sport Sci Rev 38, 128-134.

ていただき、研究者としてあるべき姿を示していただきました。心よりお礼申し上げます。また、川上研のみなさんには、口頭審査の直前までご意見いただき、自分でも納得できる発表をすることができました。学生生活からデータの解釈まで、なんでも気軽に相談できる先生や先輩方、後輩がいる研究室に所属できたことは大きな財産になりました。

　また、検者や被験者として実験に参加していただいた皆様の協力なくして、本研究を完成させることはできませんでした。本研究にご協力頂いた全ての方々に感謝致します。これからもご指導お願い致します。

　最後に、大学院に進むことを許して頂き、広島から温かく見守ってくれている家族に感謝の意を表します。家族の支えがなければ長い大学院生活を成し遂げることができなかったと思います。